공학박사 학위논문

Synthesis of metal oxide nanoparticles using supercritical fluids from a green engineering perspective

녹색 공정 관점에서의 초임계 유체를 이용한 금속산화물 나노입자의 합성

2014년 2월

서울대학교 대학원

화학생물공학부

김민수

Abstract

Synthesis of metal oxide nanoparticles using supercritical fluids from a green engineering perspective

Minsoo Kim

Supercritical Fluids Process Laboratory

School of Chemical and Biological Engineering

Seoul National University

Nano-sized materials have special and unique properties which make them useful in various fields such as optical, electrical, magnetic, and catalytic science and engineering. Industrial use of nanomaterials will require many standards such as particle size uniformity, cost-effectiveness, environmental friendliness, and reproducibility. One of the most widely known methods of nanomaterials synthesis is chemical synthetic route which involves techniques such as inverse micelles and non-hydrolytic sol-gel. These chemical synthetic methods use toxic organic solvents, involve long reaction time, require complicated and inefficient separation and purification steps, and most of all, is only available in batch mode.

This dissertation reports on the synthesis of metal and metal oxide nanoparticles using supercritical fluids. The aim is to develop more "greener" methods using supercritical fluids and natural bioresources to specifically synthesize certain metal or metal oxide nanoparticles. The advantages of the greener methods developed in this thesis are the low-cost of the reagents, short reaction time, simple reaction and downstream processing, and applicability of continuous

production using plug flow reactors.

In part one (Chapter 2), hydrothermal synthesis of cerium oxide nanocrystals was carried out with in-situ surface modification using edible vegetable oils such as soybean oil and palm oil. X-ray diffraction (XRD) patterns demonstrated that pure CeO_2 was formed. Transmission electron microscopy (TEM) showed single crystalline nature with stable dispersion. Fourier transform infrared (FT-IR) spectroscopy and thermogravimetric analysis (TGA) results confirmed the chemical adsorption of fatty acids onto the CeO_2 surfaces. This new technique employs vegetable oils as surface modifiers which are of low-cost and is abundant in nature.

The second part (Chapter 3) involves a simultaneous synthesis of biodiesel and metal (oxide) nanoparticles using supercritical methanol. The precursor for metal (oxide) nanoparticles was in nitrate form. Thus formed metal (oxide) nanoparticles catalyzed the transesterification of vegetable oil into fatty acid methyl esters (FAME, biodiesel). In addition, the catalysts also reduced the reaction temperature and time. The highest FAME yield 96.88 wt% was obtained at 250 ˚C, 350 bar, 10 min with 3 oil wt% zinc nitrate loading. FT-IR spectra revealed that the metal (oxide) nanoparticles' surfaces were modified by FAME molecules. The nanoparticles' sizes were smaller than those synthesized in neat methanol. This newly developed simultaneous synthesis process provides an economic advantage as it reduces operational temperature and time, and also produces metal compounds as by-products.

The third part (Chapter 4) utilizes glycerol as a reducing agent for synthesis of metals and metal oxide nanoparticles with supercritical water at 400 ˚C and 300 bar. Conventionally, formic acid or hydrazine were used as reducing agents for hydrothermal synthesis of inorganic materials. Formic acid and hydrazine are toxic, dangerous, chemically unstable and expensive. This chapter examines the applicability of glycerol as an environmentally benign and cheap reducing agent for hydrothermal syntheses. XRD patterns showed that silver, copper, and nickel nitrates were reduced to zero-valent metal nanoparticles. On the other hand, cobalt, iron, and manganese nitrates were partially reduced into low-valent metal oxides, which indicates glycerol's role as an anti-oxidant. The prepared metals were generally smaller in size than their corresponding metal

oxides. Glycerol is odorless, non-toxic, non-flammable, easy to handle, environmentally friendly, and readily available compared to other reducing agents. This new glycerol hydrothermal reduction method is yet, the greenest reductive materials processing in terms of chemical reagents.

The three parts of this dissertation are devoted in producing metals, metal oxides, and biodiesel using the cleanest, safest, and natural precursors such as water, methanol, vegetable oil, and glycerol. The main goal of the study is to replace the conventional chemical syntheses that use toxic and dangerous chemical reagents.

Keywords: Supercritical Fluids, Supercritical Water, Supercritical Methanol, Metal, Metal Oxide, Nanoparticles, Nanocrystals, Biodiesel, FAME, Vegetable Oil, Glycerol, Transesterification, Hydrothermal, Reduction

Student Number: 2010-30245

Table of Contents

LIST OF FIGURES

CHAPTER ONE

CHAPTER TWO

LIST OF TABLES

CHAPTER ONE

CHAPTER THREE

CHAPTER FOUR

Chapter One

Introduction

Chapter 1. Introduction

1.1 Research background

Green chemistry is about the design of chemical products and processes that reduce or eliminate the use and generation of hazardous substances [1]. Under an analogous context, green engineering is defined as the development and commercialization of industrial processes that are economically feasible and reduce the risk to human health and the environment [2]. The major concepts of green chemistry and engineering are:

- Process design for obtaining maximum yield
- Using safe and environmentally friendly raw materials
- Minimizing energy consumption of processes
- Not creating any waste to avoid waste treatment processes.

This thesis utilizes supercritical fluids technology to develop new processes for synthesizing nanomaterials from a green engineering perspective. In terms of nanoparticles production, size uniformity, size distribution, and stable dispersion are the main qualities of concern. Nanomaterials synthesis using supercritical water and supercritical methanol were carried out and characterized to show uniform nanoparticles. A comparison of the supercritical hydrothermal technique and organic solvent sol-gel method is shown in table 1.1.

Materials synthesis using supercritical fluids involve readily available common solvents such as water or methanol. The synthesis can be carried out using either batch mode or continuous plug flow mode, giving it a great advantage for large-scale production in industry. Retention time for particle crystallization is very brief, in the order of several seconds and washing step is also simple. However, there are some drawbacks such as expensive equipment costs due to high pressure of the operation. An industrial production example would be Hanwha Chemical Ltd., who produce lithium iron phosphate ($LiFePO_4$) using supercritical water in a continuous plug flow reactor. $LiFePO_4$ is used as a cathode material for secondary batteries.

	Supercritical Hydrothermal Synthesis	Organic Solvent Sol-gel
Solvents	Green solvents such as water or alcohol	Toxic and dangerous organic solvents
Production	Batch and continuous	Batch only
Process time	A few seconds to a few minutes	In the order of hours
Separation/ purification	Simple washing and drying	Complex and inefficient
Equipment	Expensive due to high pressure	Relatively less expensive

Table 1.1. A comparison between supercritical hydrothermal synthesis and organic solvent sol-gel method

1.2 Supercritical fluids

A substance is commonly known to have three phases, solid, liquid and gas. Increase in temperature melts the solid to a liquid form and further increase in temperature vaporizes the liquid into a gaseous state. Generally, pressure increases along with the increasing temperature. If the pressure was held constant in closed system and the temperature was risen, the substance will reach its critical point. A substance at above this critical point is called a supercritical fluid as shown in Figure 1.1.

Supercritical fluids behave like a gas as well as a liquid in various characteristics such as viscosity, density, diffusion coefficient, thermal conductivity, etc. A density of a supercritical fluid is liquid-like which gives high solvating power. Viscosity is gas-like so supercritical fluids can diffuse into solid materials easily without physical agitation. Supercritical fluid is in a single phase so there is no gas-liquid interface. Because there is only one phase, the pressure can be varied according to the input amount of the fluid.

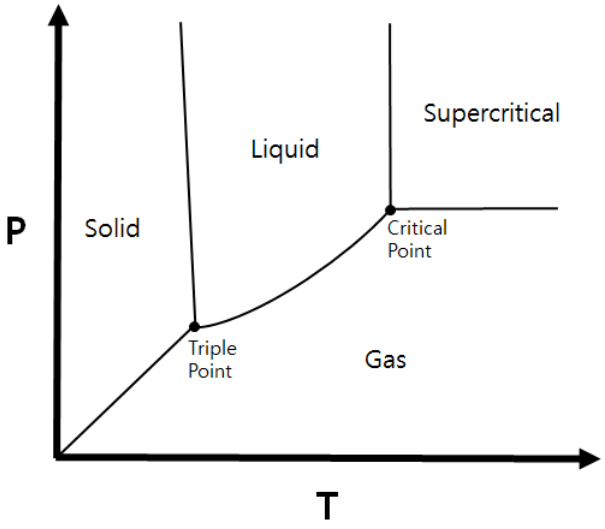

Figure 1.1. Pressure – temperature phase diagram

1.3 Typical supercritical fluids and their applications

1.3.1 Commonly used supercritical fluids

The commonly known fluids we use in a chemical engineering laboratory all have critical points. Table 1.2 shows the critical temperatures and pressures of typically used solvents. In the industry, carbon dioxide and water are mostly used for various purposes. Water and carbon dioxide are both non-toxic, cheap, and environmentally benign compared to organic solvents.

Water is the cheapest and the most abundant substance on earth. It is non-flammable, non-hazardous, and dissolves ionic substances easily. When water reaches its supercritical state, dielectric constant and ionic product constant change due to the hydrogen dissociation of the water molecule [3]. The dielectric constant of water decreases when temperature increases, as shown in Figure 1.2. Near and above the critical point, the dielectric constant of water is similar to non-polar solvents which allows near-critical water to dissolve or become miscible with organic compounds. Therefore, supercritical water can be used for gasification and oxidation of carbonaceous materials. The ionic product constant (K_w) increases along with temperature up until 250 ˚C, and then decreases drastically with further increase in temperature. This indicates that ionic reactions are better to be done in subcritical water. Water has the highest critical point which requires mass energy and high pressure equipment. Also water is a well-known oxidizer so equipment must be made of anti-oxidant materials.

Carbon dioxide has been and is the most popular solvent in supercritical fluids research. It requires relatively little energy to reach its critical point (31 ˚C, 74 bar) which is a great advantage. It is non-toxic, non-flammable and is in gaseous state at room temperature which allows easy separation from the dissolved solutes. As a gas, it is easily compressible which makes it a good fluid to recover and reuse. Gas phase CO_2 has a weak solvating power. However, when it is compressed to a liquid form or heated to a supercritical state, the increase in density increases the solvating power. Liquid or supercritical CO_2 is known to have the solvating power nearly identical to that of hexane, therefore, dissolves non-polar substances effectively.

Fluid	Critical Temperature / ˚C	Critical Pressure / bar
Water	374	221
Methanol	239	81
Ethanol	241	61
Carbon dioxide	31	74
Propane	97	43
Hexane	234	30

Table 1.2. Critical points of fluids

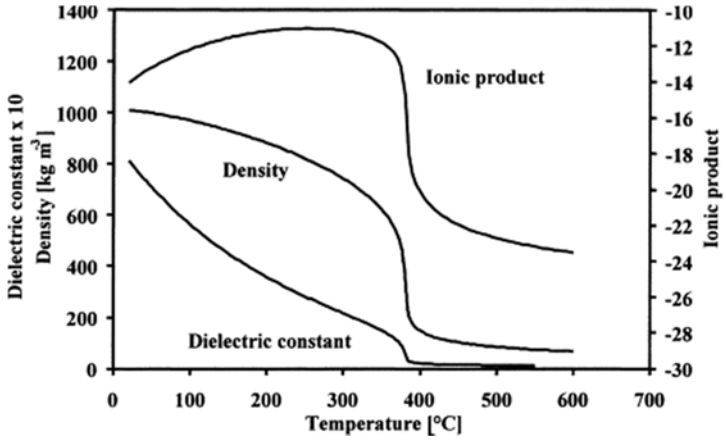

Figure 1.2. Ionic product, density, and dielectric constant of water with respect to temperature increase at 24 MPa [4]

Methanol is a cheap industrial solvent that is used in various fields of the chemical industry as a solvent and a precursor. It has very similar qualities as water but has a lower critical point which is an advantage. Supercritical methanol has low polarity like supercritical water which means it is miscible with organic compounds near the critical point. Supercritical water is a well-known an oxidizer, on the other hand, supercritical methanol is known to have reducing qualities [5]. There are some disadvantages to methanol, it is more expensive than water or CO_2, is toxic and is flammable.

1.3.2 Applications of supercritical fluids

Supercritical fluids mentioned above are all suitable for replacing the conventional techniques that use either toxic solvents or high energy such as solid state calcination methods. The main advantage is the possibility of changing temperature and pressure independently to optimize the process yield. Supercritical fluids also have excellent heat and mass transfer properties due to the single phase nature.

Supercritical fluids can have a multiple role, as a reaction solvent as well as a reactant. A typical example would be the synthesis of metal oxide nanoparticles [6]. The metal precursor (usually metal nitrate, sulfate, chloride, etc.) solution is heated up to the fluids' critical point where the solubility is drastically reduced to rapidly crystallize metal or metal oxide nanoparticles (Figure 1.3). Another example is the transesterification of vegetable oils to produce biodiesel and glycerol. The conventional production process involves methanol reflux with homogenous alkali catalysts and reaction time in the order of several hours. Using supercritical methanol, the catalyst is not required and the reaction time can be radically reduced to a few minutes. Methanol heated up to its critical point becomes miscible with vegetable oil and breaks the triglyceride molecule into three fatty acid methyl ester molecules, proving methanol as an effective solvent and a reactant.

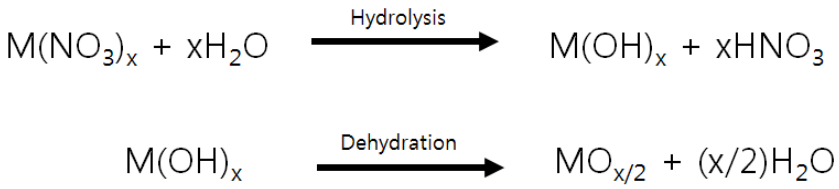

Figure 1.3. Metal oxide formation mechanism in supercritical water [6]

Extraction is the most conventional supercritical technology where supercritical carbon dioxide is the most commonly used extraction solvent [7]. When the substance to be extracted is polar, dimethyl ether or subcritical water can be used as the extraction solvent [8, 9]. For non-polar matter or macromolecules, propane or butane can be used as near-critical solvents for extraction. The advantages of supercritical carbon dioxide are the high diffusivity, low critical point and its non-toxic nature. Also because it is a gas at room temperature, product separation is simple and effective.

Crystallization (or recrystallization) of pharmaceuticals and organic compounds using near-critical carbon dioxide is a common technique. RESS (Rapid Expansion of Supercritical Solution) involves releasing the supercritical solution into the lower pressure region for the dissolved solute to crystallize. For substances that are not soluble in supercritical carbon dioxide, the supercritical carbon dioxide can be used as an anti-solvent. The solute to be recrystallized is dissolved in a solvent that is well miscible with supercritical carbon dioxide so that as the two fluids meet, the solute's solubility decreases rapidly and the solute crystallizes. This technique is the basis of ASES (Aerosol Solvent Extraction System) and SEDS (Solution Enhanced Dispersion by Supercritical Fluid).

Supercritical drying is another process using carbon dioxide. Conventional drying is simply change in the phase of the substance, from liquid to gas (Figure 1.4 No1). The evaporation creates interfacial tension which pulls the solid structures liquid is in contact with. Microstructures such as electronic devices, silica gels, and biological cell walls may be disrupted by this simple drying of solvents. To avoid this, freeze drying was developed where the liquid is frozen and is removed under reduced pressure (Figure 1.4 No2). Freeze drying avoids the liquid-gas interfacial tension but has a solid-gas boundary. Supercritical drying (Figure 1.4 No3) avoids any interfacial tension between the three phases because the supercritical state has no interface. In supercritical drying, liquid solvent is washed with liquid CO_2 which is followed by increase in temperature to turn the liquid CO_2 into supercritical CO_2. The supercritical CO_2 is slowly released into the air to leave the microstructure undamaged.

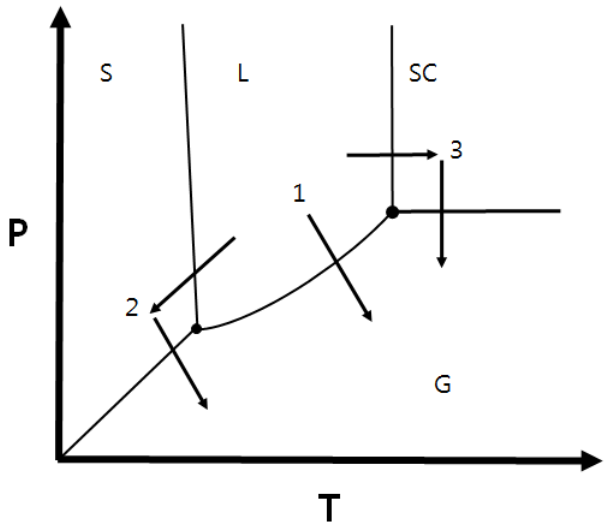

Figure 1.4. Comparison between the three drying techniques. 1 is conventional drying, 2 is freeze drying, and 3 is supercritical drying.

1.4 Dissertation overview

Since Professor Tadafumi Adschiri's invention of inorganic nanomaterials' supercritical hydrothermal synthesis [6], countless research efforts have been made and is still on going in this area. The initial hydrothermal synthesis was focused on making pure metal oxides from various forms of metal precursors such as metal nitrates, sulfates, chlorides, etc. in continuous plug flow mode. Since then, the research has shifted toward synthesizing and controlling surfaces of nanoparticles for size and shape uniformity as well as stable dispersion in an appropriate medium. The dispersion media can be either aqueous or organic depending on the surface modifying agent. The most commonly used surface modifier is carboxylic acid in the form of R-COOH where (R = 6, 10, 18). Zhang et al. synthesized perfectly dispersed ceria nanocrystals using decanoic acid as a surfactant [10]. Arita et al. used hexanoic acid, decanoic acid, and octanoic acid to modify cerium oxide surface and study the solution-state properties of three dimensional self-assembled monolayers for dispersion in various non-polar organic solvents [11]. Rangappa et al. used hexanoic acid and 1-hexylamine to change the hydrophilic surface of cobalt aluminate hydrophobic [12]. Arita et al. carried out surface modification of titanium dioxide (TiO_2) using phosphonic acids for dispersion in various organic solvents [13]. The surfactants mentioned above are highly purified reagent grade chemicals. The theme of this dissertation is green engineering and the surfactants and reducing agents used are from bioresources such as vegetable oils and glycerol which are of low-cost and is abundant in nature.

Chapter two deals with hydrothermal synthesis of cerium oxide nanocrystals with in-situ surface modification using soybean oil and palm oil. The synthesized nanocrystals were examined with XRD, TEM, FT-IR and TGA. The vegetable oils which are triglycerides were hydrolyzed into three fatty acids where the fatty acids behaved as surface modifier. Vegetable oil as new surface modifier is environmentally friendly and more economical than the conventional single component reagent grade surfactants.

Chapter three demonstrates a simultaneous synthesis of biodiesel and metal (oxides) using

supercritical methanol. Five different metal nitrates (Zn, Ce, Fe, Ni, Co) were tested for their metal (oxide) formation and catalytic activity in transesterification of rapeseed oil. The FAME contents of the biodiesel fuels were tested using GC. The synthesized nanoparticles were characterized using XRD, SEM and FT-IR. The use of metal nitrates as catalysts reduced the reaction temperature and time. Zinc nitrate was found to provide the best catalytic activity in terms of FAME yield.

Chapter four focuses on the synthesis of metals and metal oxides using supercritical water as a reaction solvent and glycerol as a reducing agent. Ag, Cu, Ni, Co, Fe and Mn were tested for their hydrothermal reducibility. XRD patterns confirmed that silver, copper and nickel nitrates were completely reduced to zero-valent metal nanoparticles. Cobalt, iron and manganese nitrates were partially reduced into low-valent metal oxides. SEM images showed that the reduced metals and metal oxides were smaller that the metal oxides hydrothermally synthesized without glycerol. The difference in reduction behavior is explained using their reduction potentials.

Chapter Two

Vegetable oil aided hydrothermal synthesis of cerium oxide nanocrystals

Chapter 2. Vegetable oil aided hydrothermal synthesis of cerium oxide nanocrystals

2.1 Introduction

The recent trend of research in metal oxide nanocrystals is heavily focused on reducing size and modifying morphology due to the unique properties at nano-scale such as quantum size effect, change in optical properties and tuning of band-gap [14]. Cerium oxide (ceria, CeO_2) is a versatile material used in various applications such as catalysis, solid oxide fuel cells (SOFC), chemical mechanical polishing (CMP), ultraviolet light blocking, insulators, etc. Various synthetic methods have been exploited to obtain nano-sized ceria crystals such as aqueous precipitation, sol-gel, mechanochemical, pyrolysis, thermal decomposition, sonochemical, solvothermal, etc [15]. Our method of choice was hydrothermal synthesis using supercritical water (SCW) with the aid of vegetable oils as surfactants to modify nanocrystal surfaces and prevent particle aggregation. SCW as a solvent is cheap, readily available, environmentally benign, easier to waste-treat than organic solvents and has proven continuous producibility which is already applied in the industry [16, 17].

Traditionally in solution chemistry, surfactants such as oleic acid, decanoic acid, hexanoic acid and oleylamine were employed to modify the size, morphology and surface characteristics of ceria nanocrystals. Various sizes and shapes such as spherical, cubic, octahedron, rod, wire and nanosheets with surface modification have been obtained [18-20]. These single component reagent grade surfactants are expensive due to various high temperature reactions and purification processes involved in obtaining high purity [21]. This research was aimed to study the surface modification of metal oxide nanocrystals using vegetable oils such as soybean oil or palm oil which are cheap and readily available in mass quantities compared to the aforementioned single component surfactants. Vegetable oils or animal fats are mixtures of triglycerides where the fatty acids vary in their carbon chain length and in the number of double bonds [22]. As the oil and

water mixture is heated, triglyceride molecules are hydrolyzed to yield three moles of fatty acids and one mole of glycerol where the free fatty acid molecules can act as surfactants that that adsorb onto nanocrystal surfaces.

2.2 Experimental

Cerium hydroxide ($Ce(OH)_4$) was purchased from Aldrich. Ottogi soybean oil was purchased from a local grocery store and palm oil was generously supplied by Dongnam Oil & Fats Co., Ltd, Korea. Fatty acid compositions of the oils used were provided by the oil suppliers and are as follows. Soybean oil: palmitic (16:0) 11%, stearic (18:0) 5%, oleic (18:1) 29%, linoleic (18:2) 50% and linolenic (18:3) 5%. Palm oil: myristic (14:0) 3%, palmitic (16:0) 41%, stearic (18:0) 5%, oleic (18:1) 42% and linoleic (18:2) 9%. Water was purified by Millipore, Milli-Q Advantage A10. All chemicals were used as received without further purification. 0.17 g of cerium hydroxide, 1.4 g of either soybean oil or palm oil and 6.6 ml of deionized water were placed in a SUS316 reactor of 23 ml inner volume. The hydrothermal reaction was carried out using a thermostated salt bath at 400 °C and 300 bar. (Salt bath content: $NaNO_3 – KNO_3 – Ca(NO_3)_2$ = 46:24:30) The reactor was constantly shaken for 10 minutes which was followed by rapid quenching in a water bath at room temperature. The resulting powder was isolated by centrifugation and washed three times with ethanol and hexane to remove any remaining organic residues. The finally obtained products were dried in a vacuum oven at 80 °C for 24 hours. The obtained solid products were characterized by X-ray diffraction (XRD), transmission electron microscopy (TEM), high resolution transmission electron microscopy (HR-TEM), Fourier transform infrared spectroscopy (FT-IR) and thermo gravimetric analysis (TGA). XRD patterns were obtained using Rigaku D/Max-3C diffractometer with Cu Kα radiation. TEM and HR-TEM images were taken from JEOL model JEM-3010. Sample solutions were dried on 300 mesh copper grids with carbon reinforcement prior to TEM analysis. FT-IR spectroscopy was conducted by Thermo Scientific model Nicolet 6700. TGA was analyzed using TA Instruments model Q-5000 IR.

2.3 Results and discussion

Initially, a clear two-phase layer is formed when the reactor is filled up with water, cerium hydroxide powder and vegetable oil. As the temperature is increased, the heated water rapidly hydrolyzes triglyceride molecules to release fatty acids which are soluble in subcritical water, making the whole system homogenous. Simultaneously cerium hydroxide dehydrates to form cerium oxide and the released fatty acids chemically adsorb in a selective manner on the ceria nanocrystals' surfaces to retard crystal growth, thus controlling the nanocrystal size and morphology [10]. The whole process is illustrated in Figure 2.1. A two phase mixture exists when the reaction is complete, the upper layer containing nanocrystals dispersed in fatty acid phase and the lower layer containing glycerol dissolved in water. Glycerol is a commonly used raw material for pharmaceutical, medical and personal care applications. The lower water phase solution can be collected for glycerol separation and purification in a large scale process.

The XRD patterns of the synthesized ceria nanocrystals showed cubic fluorite structure (JCPDS Card No. 34-0394), shown in Figure 2.2. The XRD patterns for soybean oil assisted nanocrystals showed that pure cerium oxide was formed (Figure 2.2b). However, for the case of palm oil assisted nanocrystals (Figure 2.2c), a small residual free fatty acid peak at 21.3° region was observed. It was found that after the hydrothermal synthesis, the removal of free fatty acid residues is more difficult for palm oils than that of soybean oils. This is thought to be caused by the fact that palm oil has higher degree of alkyl chain saturation than soybean oil. Palm oil is semi-solid at room temperature whereas soybean oil is liquid.

Figure 2.3 is a collection of TEM and HR-TEM images of the synthesized nanocrystals. The unmodified ceria nanocrystals were aggregated with quasi-spherical shape (Figure 2.3a). The average particle size calculated by Scherrer equation was 9.2 nm. Ceria nanocrystals surface-modified by soybean oil and palm oil were well-dispersed (Figures 2.3b and 2.3c, respectively) having a size distribution of 7-10 nm base length. The HR-TEM images of unmodified, soybean oil modified and palm oil modified nanocrystals showed parallel lattice patterns demonstrating the high crystallinity and single-crystalline nature (Figures 2.3d, 2.3e and 2.3f, respectively).

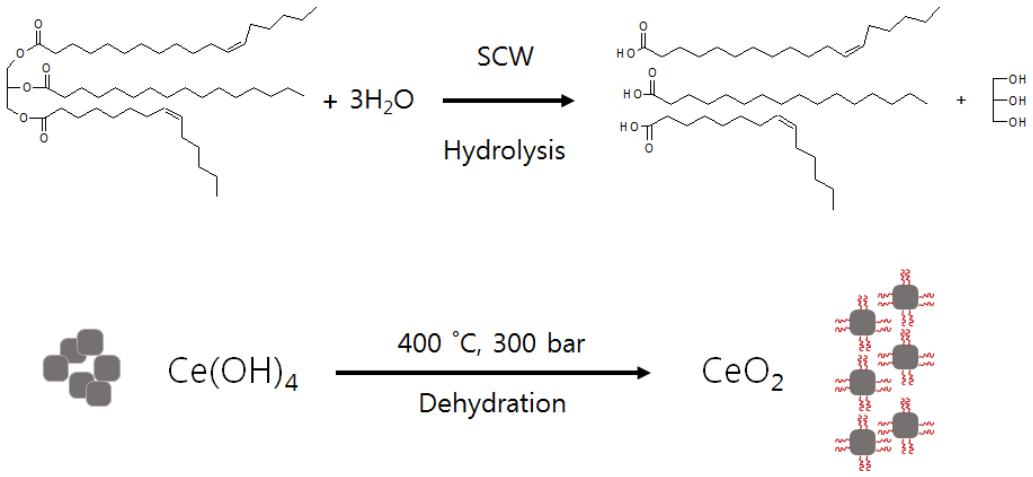

Figure 2.1. An illustration of reactions occurring when vegetable oil and cerium hydroxide reacts with SCW

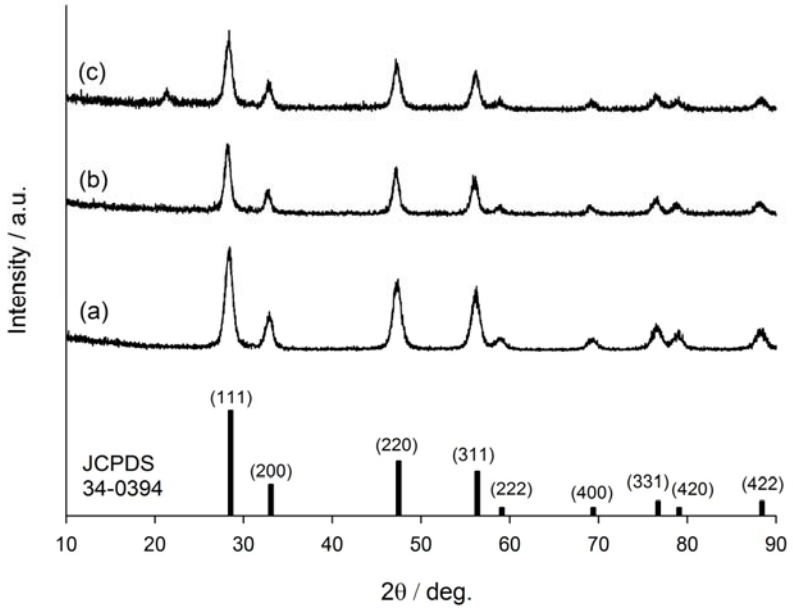

Figure 2.2. XRD patterns of cerium oxide nanocrystals synthesized in supercritical water at 400 °C: (a) Without any surface modifiers, (b) with soybean oil and (c) with palm oil

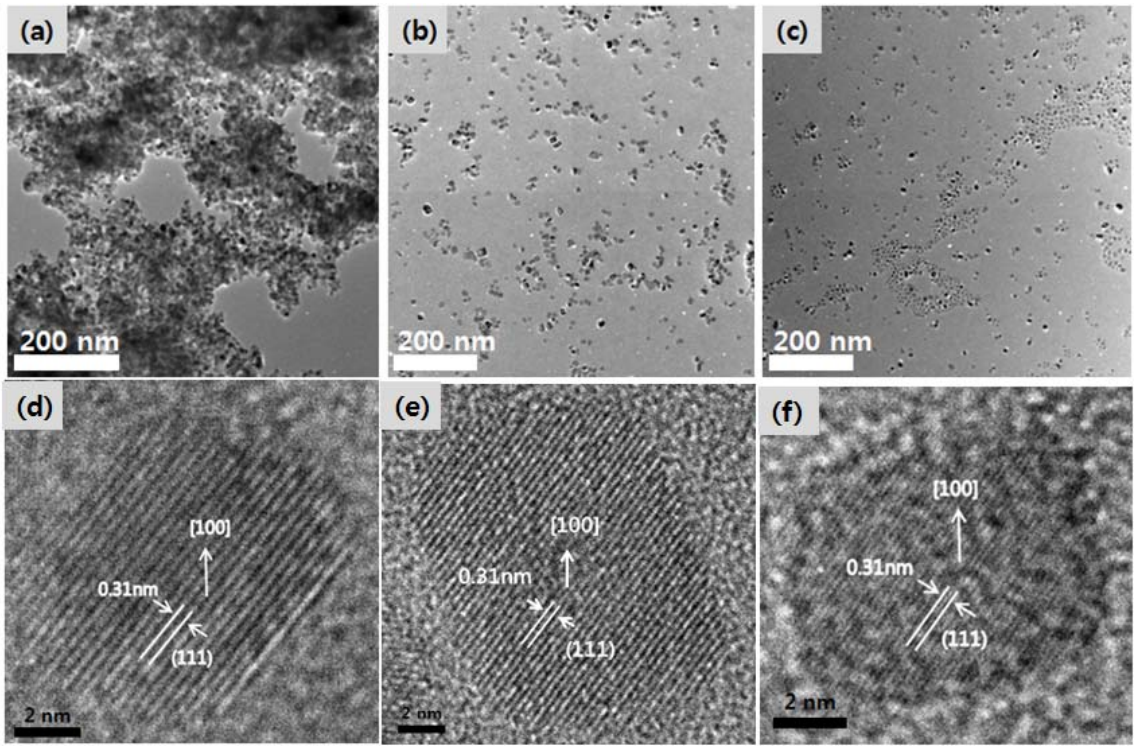

Figure 2.3. TEM and HR-TEM images of cerium oxide nanocrystals synthesized in supercritical water at 400 °C: (a and d) without any surface modifiers, (b and e) with soybean oil (c and f) with palm oil

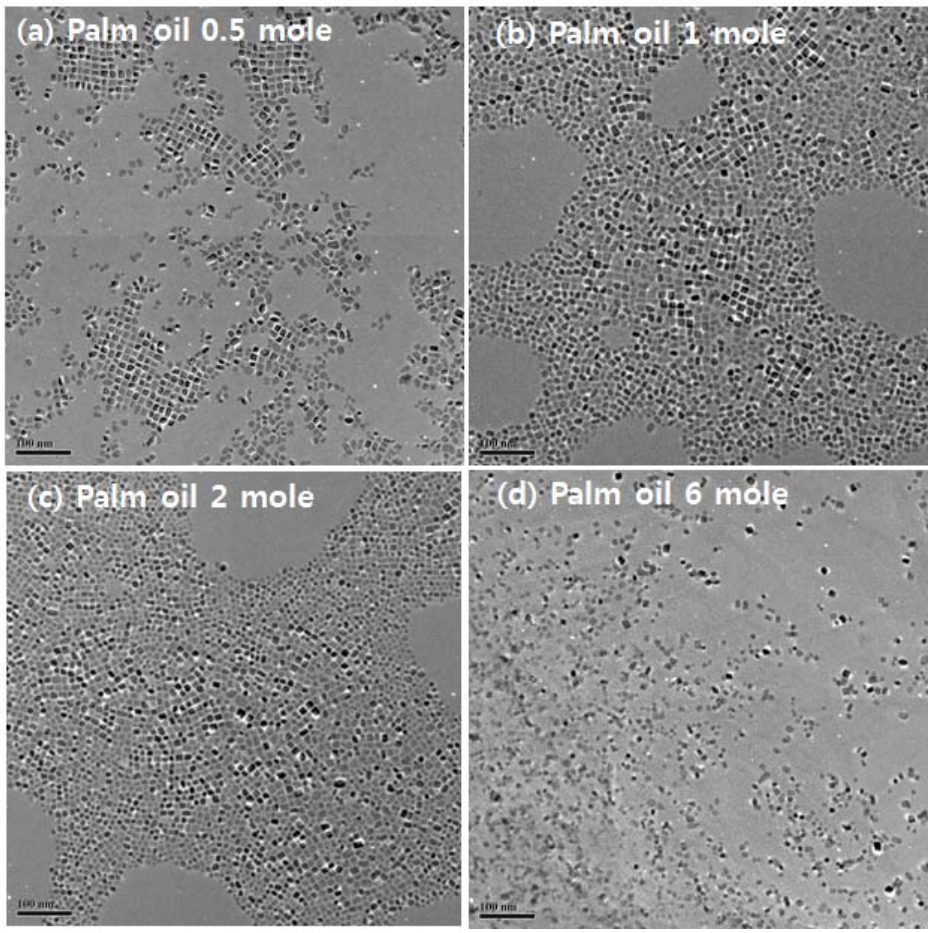

Figure 2.4. TEM images of cerium oxide nanocrystals with different amounts of palm oil added relative to the metal precursor amount: (a) 0.5 mole, (b) 1 mol, (c) 2 mol, and (d) 6 mol

Amount of vegetable oil necessary for stable dispersion was checked using palm oil. Figure 2.4 shows the TEM images of cerium oxide nanocrystals surface modified using 0.5, 1, 2 and 6 moles of palm oil relative to the metal precursor cerium hydroxide. CeO_2 nanocrystals were perfectly dispersed and self-assembled when 0.5 to 2 moles of palm oil was used. However, when 6 moles of palm oil was used, the nanoparticles did not self-assemble in stable monolayers. There are two possible explanation for this. One is the difficulty in washing off the fatty acids due to the excess amount of palm oil used. The other reason would be the overloading of palm oil which causes the entire surface of cerium oxide (regardless of the surface stability) to be bound by the fatty acids.

FT-IR studies were conducted to characterize the surface-bound fatty acids of cerium oxide and the resulting spectra are shown in Figure 2.5. There were no characteristic peaks found for the synthesis without any modifiers, shown in Figure 2.5a. When either soybean oil or palm oil were used to aid the synthesis (Figure 2.5b and 2.5c, respectively), following surface-bound fatty acid peaks were observed; $-CH_3-$ asym str at 2955 cm^{-1}, $-CH_2-$ asym str at 2915 cm^{-1}, $-CH_2-$ sym str at 2847 cm^{-1} and -COO str at 1544 cm^{-1}. These peaks suggest that the carboxylate group of the fatty acid molecules were chemically bonded on the surfaces of synthesized nanocrystals [23]. Soybean oil and palm oil were also analyzed with infrared and the resulting spectra are shown in Figure 2.5d and 2.5e, respectively. Both oils had a characteristic 'unbound' carbonyl peak at 1745 cm^{-1} which were shown to disappear when the fatty acids chemically adsorbed onto CeO_2. It appears that the hydrothermal reaction that reaches conditions up to supercritical region allows rapid hydrolysis of the triglycerides and the chemical bond formation between the released fatty acids and the nanocrystal surfaces resulting in nanocrystal surface stabilization. An increase in peak intensity when palm oil was used instead of soybean oil suggests the existence of residual fatty acids which is consistent with XRD data shown above.

TGA was performed to quantitatively investigate the presence of organic modifiers on nanocrystal surfaces. Samples were heated to 800 °C at a rate of 10 °C/min under constant flow of nitrogen and the resulting thermograms are shown in Figure 2.6. Unmodified nanocrystals had a weight reduction of 3.5% at 800 °C (Figure 2.6a). This small decrease is thought to be caused

by the removal of hydroxyl groups at the surface. Nanocrystals synthesized with the aid of soybean oil and palm oil had lost 22% and 53% of its original weight at 800 °C, respectively. There are two possible reasons for the large weight decrease in palm oil assisted nanocrystals. One is due to the existence of residual fatty acids that were also shown in the XRD patterns, Figure 2.2 (c). Another explanation is the higher nanocrystal surface coverage of palm oil derived fatty acids. This is consistent with the fatty acid composition data where palm oil has higher degree of alkyl chain saturation which provides less steric hindrance when chemically bonded onto nanocrystal surfaces. Our future work will focus on the complete removal of residual organic matter from hydrothermally synthesized oxide nanomaterials.

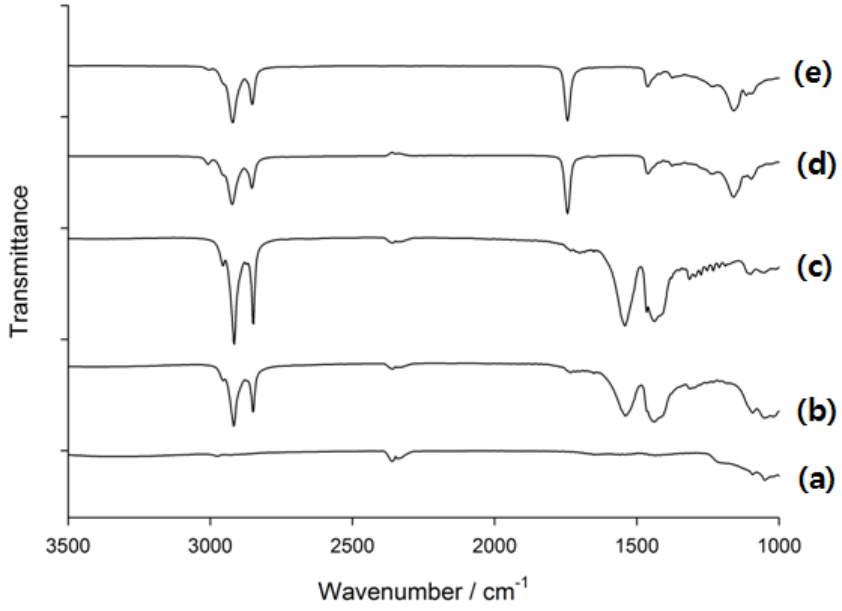

Figure 2.5. FT-IR spectra: (a), (b), (c) are CeO_2 synthesized without any surface modifiers, with soybean oil and with palm oil, respectively and (d) and (e) are soybean oil neat and palm oil neat, respectively

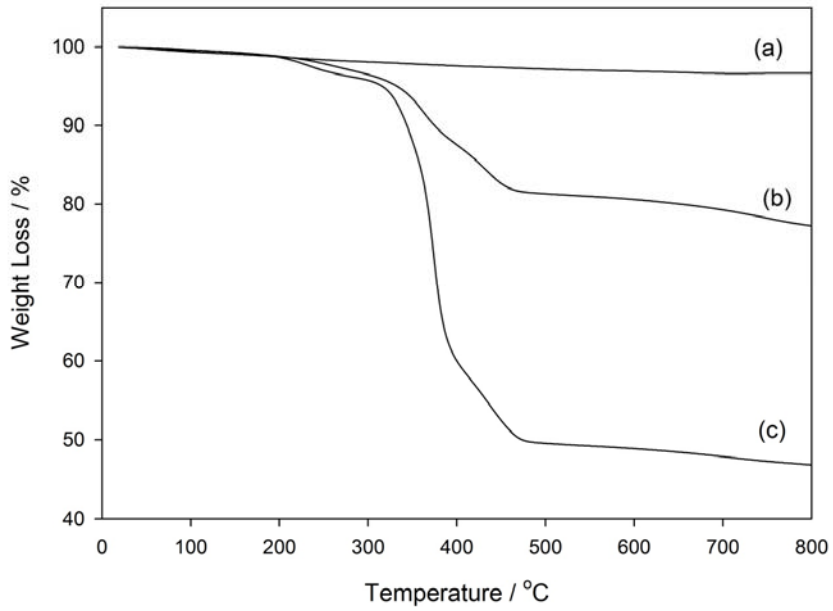

Figure 2.6. TGA thermograms of cerium oxide nanocrystals synthesized in supercritical water at 400 °C: (a) Without any surface modifiers, (b) with soybean oil and (c) with palm oil

2.4 Summary

Well-dispersed cerium oxide nanocrystals were successfully synthesized and surface-modified using cheap edible oils. Fatty acids from either soybean oil or palm oil were successfully bonded to ceria nanocrystals' surfaces for stable surface modification and dispersion. Our novel method of synthesis was proven to be facile, highly economical and environmentally friendly. Soybean oil and palm oil are not the only suitable surface modifiers, all forms of triglycerides from vegetable oils to animal fats are possible candidates for such purpose.

Chapter Three

Simultaneous synthesis of biodiesel and metal oxide nanoparticles using supercritical methanol

Chapter 3. Simultaneous synthesis of biodiesel and metal oxide nanoparticles using supercritical methanol

3.1 Introduction

Biodiesel consists of fatty acid methyl esters (FAMEs), which are the products of the transesterification of vegetable oils or animal fats using alcohol (Figure 3.1). It is being explored as an energy source for the future, owing to its nontoxicity, biodegradability, and renewability. Typically, biodiesel is free from sulfur, aromatics, particulates, and carcinogenic substances, components that are all present in petroleum diesel combustion emissions [24]. With the prices of crude oil constantly increasing, the renewability of biodiesel is a great advantage because any type of triglyceride oil can be used to produce biodiesel, including animal fats, microalgae, and waste cooking oils.

Currently known methods for synthesizing biodiesel involve the use of either homogeneous or heterogeneous catalysts, or supercritical methanol [25]. Methods employing homogeneous catalysts, which are used widely in the industry, require the use of acids or alkalis as catalysts. Despite being produced on a large scale, homogeneous catalysts are not reusable, produce a great amount of wastewater, and lead to a deterioration in the quality of glycerol since they dissolve in it. On the other hand, the use of heterogeneous catalysts results in simplified synthesis and purification processes that are economically attractive, since these catalysts are reusable. However, even though heterogeneous catalysts have some advantages over homogenous catalysts, they also have a few limitations that need to be addressed. First, while solid catalysts are known to be reusable, their activity slowly diminishes with repeated use. Second, the three-phase nature of the oil-methanol-catalyst mixture (liquid-liquid-solid) results in limitations with respect to mass transfer, requiring a more sophisticated catalyst design and vigorous agitation. Third, heterogeneous catalysts are composed of inorganic metals/metal oxides and are more expensive than homogeneous catalysts [26]. The supercritical methanol method developed by Saka et al.,

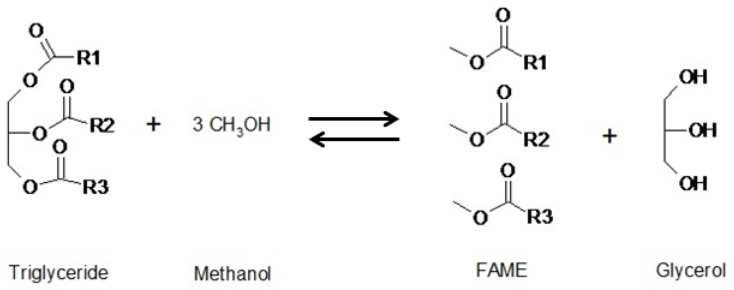

Figure 3.1. Transesterification of triglyceride with methanol

does not require a catalyst and results in shorter reaction time than those of conventional catalytic processes [27]. In addition, because this process does not require a catalyst or downstream separation/purification, it is more cost effective than the other methods. A reduction in the reaction time is another advantage associated with this method; while catalytic transesterification takes several hours, depending on the temperature, the supercritical methanol method requires only a few minutes. However, the extremely high temperature and pressure conditions involved require expensive equipment. In order to alleviate the severe operating conditions, Yoo et al. applied metal oxide catalysts with supercritical and subcritical methanol to synthesize biodiesel [28]. Yoo et al. tested five different metal oxides and concluded that zinc oxide was the optimum catalyst for reducing the reaction temperature and time involved in biodiesel synthesis. In this chapter, I took a new approach and attempted to synthesize biodiesel and metal oxide simultaneously using supercritical methanol. I introduced various metal nitrate as a precursor for synthesizing metal oxides in the transesterification of rapeseed oil. The synthesized metal oxides could be used for two purposes: as a catalyst for increasing the FAME yield of the biodiesel and as an inorganic nanoparticle product on its own.

Synthesis of metals and metal oxides using supercritical and subcritical methanol was attempted by many researchers. Kim et al. reported the synthesis of silver (Ag), copper (Cu), and nickel (Ni) nanoparticles using supercritical methanol and ethanol [5]. Shin et al. synthesized cobalt (Co) nanoparticles [29] and Veriansyah et al. synthesized magnetite (Fe_3O_4) nanoparticles [30] using supercritical methanol. Synthesis of metal particles using supercritical methanol does not require a reducing agent since methanol behaves as a reducing agent as well as a reaction medium.

In this chapter, metals and metal oxides were synthesized in supercritical methanol along with vegetable oils for FAME formation. Figure 3.2(a) shows the schematic block diagram of the transesterification of vegetable oil using supercritical methanol. This process yielded two products: biodiesel and glycerol. I have introduced a metal precursor into this process to increase the FAME yield and to produce metal oxide nanoparticles as a byproduct. After the introduction of the precursor, the process yielded three products: biodiesel, glycerol, and metal oxide in the

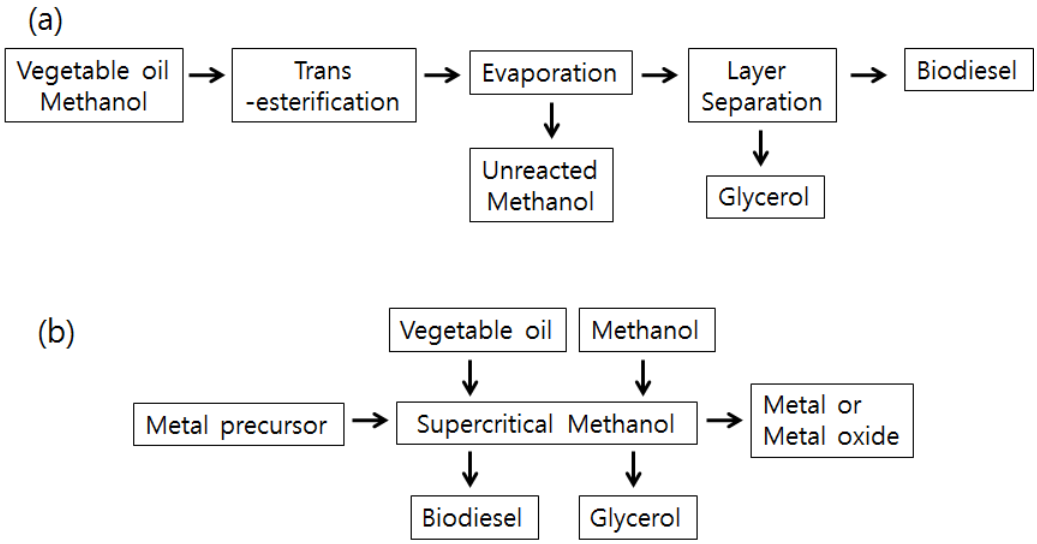

Figure 3.2. Block diagrams (a) showing the transesterification of rapeseed oil using supercritical methanol and (b) showing the simultaneous synthesis of biodiesel and metal or metal oxide nanoparticles using supercritical methanol

form of nanoparticles, with the in-situ formed metal oxide behaving as a catalyst. A schematic block diagram of the latter process is shown in Figure 3.2(b).

3.2 Experimental

3.2.1 Materials

The rapeseed oil used in this study was Beksul canola oil and methanol was obtained from J. T. Baker. Methyl heptadecanoate and n-heptane were purchased from Fluka and Junsei, respectively, for use as analytical standard in gas chromatography (GC) analysis. Zinc nitrate hexahydrate and cerium nitrate hexahydrate were purchased from Samchun Pure Chemical. Iron nitrate nonahydrate was purchased from Sigma Aldrich. Nickel nitrate hexahydrate and cobalt nitrate hexahydrate were obtained from Hayashi Pure Chemical and Junsei, respectively.

3.2.2 Experimental procedure

The transesterification reactions of rapeseed oil were carried out in a stainless steel (SUS316) reactor with an inner volume of 23 ml. A thermostat-monitored salt bath containing a mixture of metal salts (Salt bath content: $NaNO_3$ – KNO_3 – $Ca(NO_3)_2$ = 46:24:30) was used to heat the reactor to the desired reaction temperature. Certain amounts rapeseed oil and methanol were introduced into the reactor to fit the desired reaction pressure and the precursor mole ratio, which were calculated using methanol density data from NIST Chemistry Webbook [http://webbook.nist.gov/chemistry/]. For the simultaneous synthesis of biodiesel and metal compounds, the amount of metal nitrate added was 3 wt% of rapeseed oil. After loading all the precursors, the reactor was tightly sealed and immersed into the molten salt bath preheated to the reaction temperature. The reactor was shaken using a mechanical shaker for 1 – 20 minutes before being rapidly quenched in cool water to terminate the reaction.

The reaction product was dried in a vacuum oven at 60 °C to remove excess methanol. The product was of three phases, biodiesel on the top layer and glycerol in the bottom layer with metal

compound nanoparticles. The top layer was carefully collected for GC analysis to determine the FAME contents of the products. The bottom layer was repeatedly washed with methanol to remove glycerol and the finally obtained particles were dried in a vacuum oven at 60 °C for physical study.

3.2.3 Characterization

The biodiesel samples were analyzed using the test methods described in BS EN14103 [31]. The FAME yields in the various crude biodiesel samples formed under different process conditions were determined using a gas chromatograph (Agilent, HP6890) having a capillary column (Agilent, HP-INNOWAX) with the dimensions of 30 m × 0.32 mm × 0.25 μm and a flame-ionization detector (FID).

The fabricated metal oxide nanoparticles were analyzed using X-ray diffraction (XRD), scanning electron microscopy (SEM), transmission electron microscopy (TEM), and Fourier transform infrared (FT-IR) spectroscopy. The XRD patterns were collected using Rigaku D/Max-3C diffractometer with Cu Kα radiation. The SEM images were obtained using a Carl Zeiss Auriga and the TEM images were taken from JEOL JEM-3010. The sample solutions were dried on carbon-reinforced 300 mesh copper grids prior to the TEM analysis. The FT-IR spectra were obtained using a Thermo Scientific Nicolet 6700 spectrometer.

3.3 Results and discussion

3.3.1 The FAME yields of the various biodiesel samples

The transesterification of vegetable oils using supercritical methanol is dependent on four major parameters: the temperature, pressure, methanol-to-oil mole ratio, and reaction time. In this study, the temperature (250–400 °C), pressure (250–350 bar), and reaction time (1–20 min) were varied. The methanol-to-oil mole ratio was fixed at 40, on the basis of data from previous studies [28, 32]. Table 3.1 lists the conditions used for the transesterification of rapeseed oil. The amounts of

No.	Pressure (bar)	Temp. (°C)	Reaction time (min)	Rapeseed oil (g)	Methanol (g)	FAME yield (%)	No.	Pressure (bar)	Temp. (°C)	Reaction time (min)	Rapeseed oil (g)	Methanol (g)	FAME yield (%)
1	250	250	1	6.11	8.89	2.45	29	300	400	1	3.36	4.90	87.82
2	250	250	5	6.11	8.89	15.35	30	300	400	5	3.36	4.91	79.71
3	250	250	10	6.11	8.89	19.84	31	300	400	10	3.37	4.91	63.07
4	250	250	20	6.11	8.90	22.55	32	300	400	20	3.36	4.92	56.37
5	250	300	1	5.02	7.31	13.69	33	350	250	1	6.27	9.23	1.09
6	250	300	5	5.03	7.32	16.43	34	350	250	5	6.29	9.22	1.61
7	250	300	10	5.02	7.31	70.58	35	350	250	10	6.30	9.23	18.83
8	250	300	20	5.03	7.31	94.80	36	350	250	20	6.29	9.22	28.60
9	250	350	1	3.65	5.32	80.36	37	350	300	1	5.65	8.23	3.91
10	250	350	5	3.66	5.33	90.98	38	350	300	5	5.66	8.23	14.94
11	250	350	10	3.66	5.33	91.29	39	350	300	10	5.64	8.23	26.55
12	250	350	20	3.66	5.32	88.75	40	350	300	20	5.66	8.23	92.73
13	250	400	1	2.80	4.05	86.87	41	350	350	1	4.71	6.86	70.81
14	250	400	5	2.79	4.05	79.89	42	350	350	5	4.71	6.86	92.99
15	250	400	10	2.79	4.07	67.22	43	350	350	10	4.71	6.87	91.46
16	250	400	20	2.78	4.06	55.42	44	350	350	20	4.71	6.87	88.95
17	300	250	1	6.27	9.12	4.46	45	350	400	1	3.87	5.62	90.61
18	300	250	5	6.26	9.11	5.90	46	350	400	5	3.87	5.63	77.47
19	300	250	10	6.28	9.12	9.50	47	350	400	10	3.86	5.64	64.02
20	300	250	20	6.28	9.11	32.00	48	350	400	20	3.86	5.64	52.99
21	300	300	1	5.37	7.86	7.03	49*	350	250	10	6.38	9.30	96.88
22	300	300	5	5.39	7.86	15.36	50*	350	300	10	5.65	8.23	93.92
23	300	300	10	5.38	7.87	36.37	51*	350	350	10	4.70	6.86	88.79
24	300	300	20	5.37	7.87	96.33	52*	350	300	1	5.65	8.23	91.84
25	300	350	1.00	4.28	6.23	55.04	53*	350	300	5	5.63	8.22	92.95
26	300	350	5.00	4.29	6.24	81.06	54*	350	300	10	5.65	8.23	93.92
27	300	350	10.00	4.27	6.22	92.39	55*	350	300	20	5.67	8.22	92.63
28	300	350	20.00	4.26	6.22	89.65							

Table 3.1. Experimental conditions for the synthesis of biodiesel using rapeseed oil. * means the zinc nitrate was added

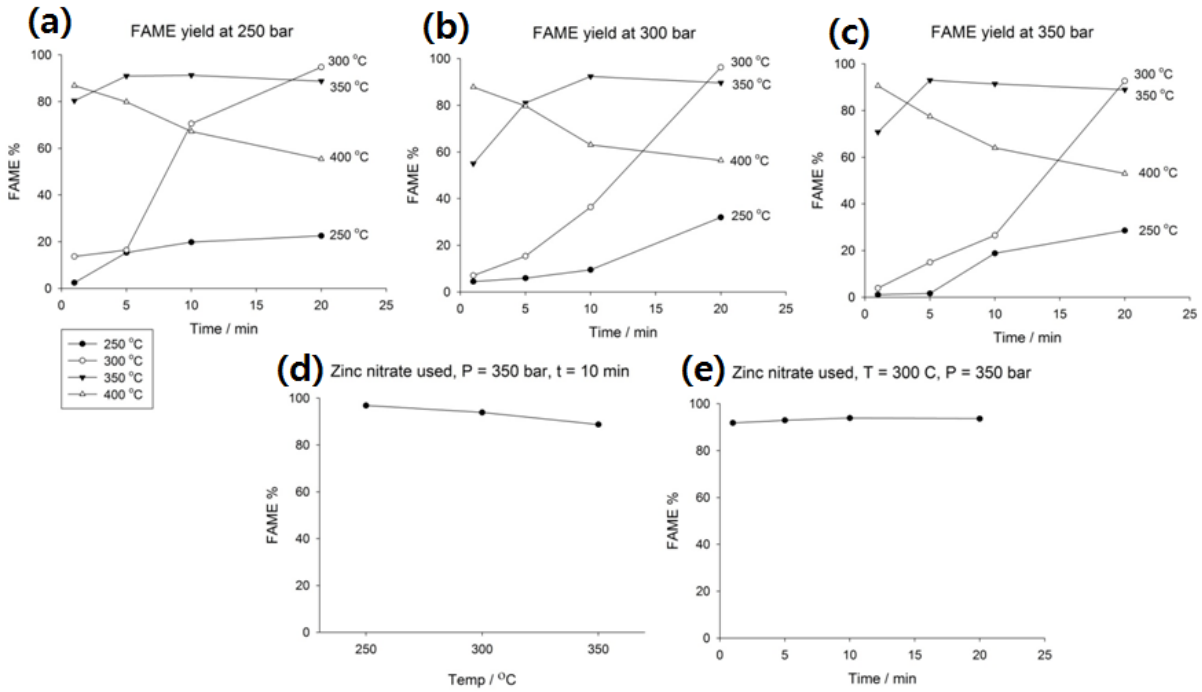

Figure 3.3. GC results from various experimental conditions. (a), (b), and (c) are the FAME yield curves for the biodiesels synthesized using neat supercritical methanol with the temperature, pressure, and reaction time being varied. (d) And (e) shows the FAME yield curves for the biodiesels synthesized using supercritical methanol and zinc nitrate. In the case of (d), the temperature was varied, with the other parameters remaining constant, and for (e), the reaction time was varied at 300 ˚C. The methanol-to-rapeseed oil mole ratio was kept constant at 40 in all the cases

rapeseed oil and methanol to be loaded were calculated on the basis of available methanol density data as explained in the Experimental section. Figure 3.3 shows the FAME yields when the experimental parameters were varied. The curves in Figs. 3.3(a), 3.3(b), and 3.3(c) are the FAME yields for different reaction times and temperatures with the pressure being 250 bar, 300 bar, and 350 bar, respectively. The reaction temperature and time were the major factors influencing the FAME yield, and this was consistent with previously reported results [33]. For temperatures of 250 °C and 300 °C, an increase in the reaction time increased the FAME yield directly. At 350 °C and any given pressure, a reaction time of 5 to 10 min resulted in the highest FAME yield, and increasing the reaction time further to 20 min reduced the FAME yield slightly. At 400 °C, for any given pressure, the FAME yield decreased drastically with an increase in the reaction time. This decrease in the FAME yield at temperatures of 350–400 °C was due to the thermal degradation of rapeseed oil. Rapeseed oil is highly unsaturated [34], and double bonds are known to be more susceptible to thermal degradation [27].

Figures 3.3 (d) and (e) show the FAME yields when zinc nitrate was used in-situ for the transesterification. In the case of the yield curve shown in Figure 3.3 (d), the temperature was varied while the pressure was fixed at 350 bar, the reaction time at 10 min and 3 oil wt% zinc nitrate added. The maximum FAME yield was 96.88%, which was obtained at a temperature of 250 °C, pressure of 350 bar, and a reaction time of 10 minutes. When the other parameters were held constant, an increase in the temperature to either 300 °C or 350 °C decreased the FAME yield slightly. The added zinc nitrate was converted into zinc oxide nanoparticles by the solvothermal reaction in supercritical methanol and was characterized, as described in the next section. Heterogeneous metal-oxide catalysts are well suited for use in the transesterification of oils [24, 28]. Therefore, a 10 min reaction time was more than sufficient and an increase in the temperature caused the FAMEs to thermally degrade. In another case, the reaction time was varied while the temperature was maintained at 300 °C with the pressure fixed at 350 bar, and 3 oil wt% of zinc nitrate added. The results for this case are shown in Figure 3.3 (e). An increase in the reaction time from 1 min to 20 min had only a small effect on the total FAME yield, which was

between 91–94%. Therefore, zinc nitrate can be used in-situ to reduce the operational temperature and reaction time during the transesterification of oils using supercritical methanol.

As mentioned in the Introduction, heterogeneous catalysts gradually lose their activity with time due to poisoning. However this is not the case in our study because fresh zinc nitrate is supplied for every new batch reaction. Therefore, a high FAME yield is guaranteed throughout the entire production process.

3.3.2 Characterization of ZnO nanoparticles

The introduction of zinc nitrate during the supercritical methanol transesterification process resulted in the formation of zinc oxide nanoparticles. The nitrate group in zinc nitrate is released as nitric acid during the reaction and exists in glycerol phase. For comparison, zinc oxide was also synthesized using methanol only. Figure 3.4 shows the XRD patterns of the ZnO nanoparticles synthesized during transesterification (a) and those using only methanol (b), both at 300 °C, 350 bar with the reaction time being 10 min. The XRD patterns of both types of ZnO nanoparticles matched well with the JCPDS Card No. 79-0208 and exhibited good crystallinity. Comparing the two patterns, it was found that the peaks of the ZnO nanoparticles formed during the biodiesel synthesis were much smaller in magnitude and broader, indicating that they were smaller in size than those fabricated using only methanol. The particle size reduction is caused by the existence of rapeseed oil which creates mass transfer resistance during ZnO crystallization in the methanol medium.

Figure 3.5 shows the SEM and TEM images of the ZnO nanoparticles synthesized in pure methanol (a, b, c) and those formed during transesterification (d, e, f). The ZnO nanoparticles formed in neat methanol were spherical, with a size distribution range of 1.6 – 1.9 μm. The ZnO nanoparticles produced during transesterification had a shape similar to that of round rice crackers and a size distribution of 600 – 900 nm. The fact that the nanoparticles formed during transesterification were smaller in size was consistent with the results of the XRD patterns. The TEM images of the ZnO nanoparticles showed that primary particles of 1.8 μm in size were

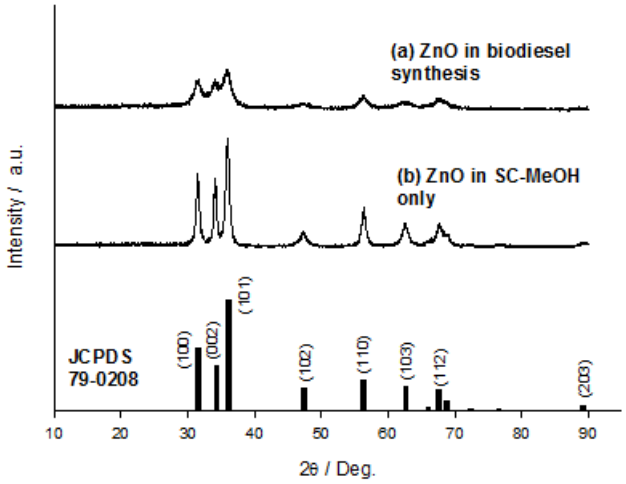

Figure 3.4. XRD patterns of the ZnO nanoparticles (a) synthesized during the transesterification of rapeseed oil in supercritical methanol at 300 °C and 350 bar over a period of 10 min and (b) synthesized in neat supercritical methanol under identical conditions

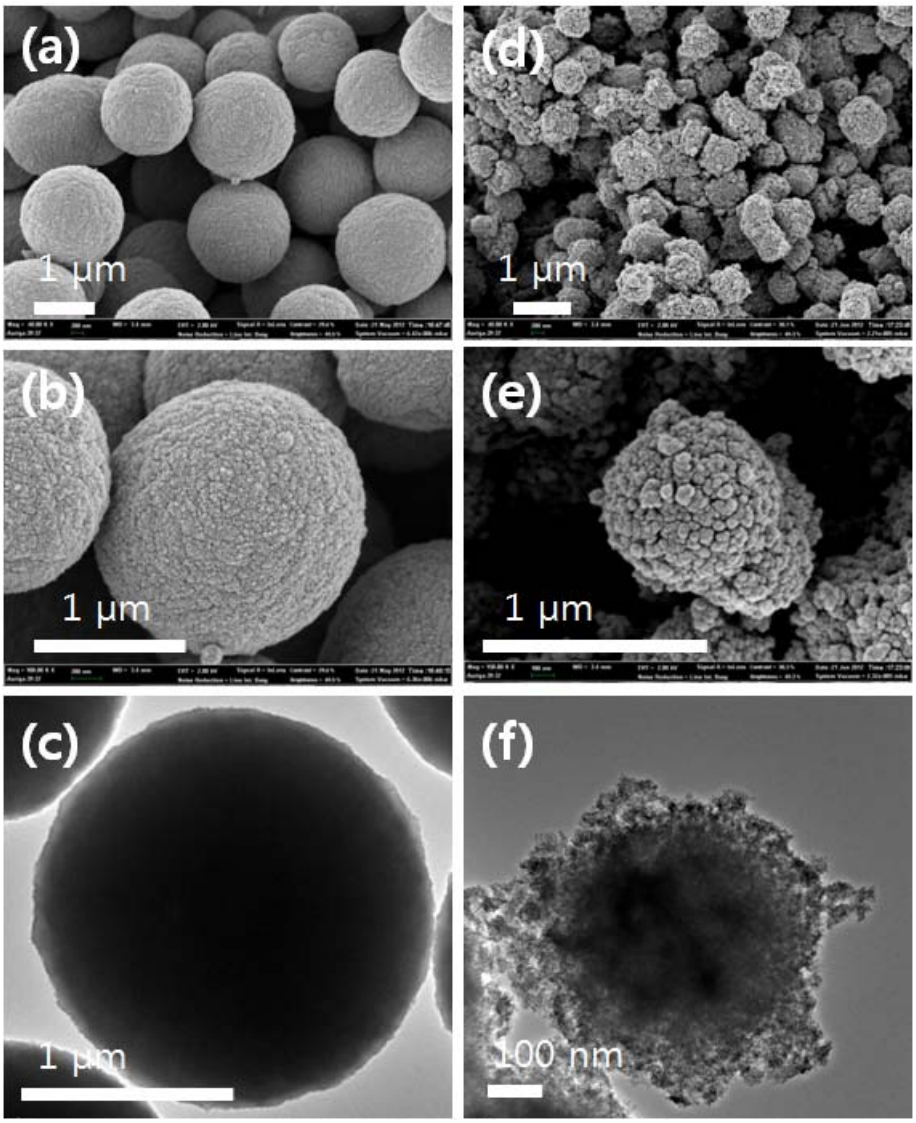

Figure 3.5. SEM and TEM images of the ZnO nanoparticles synthesized in neat supercritical methanol at 300 °C and 350 bar over a period of 10 minutes (a), (b), (c) and ZnO synthesized during the transesterification of rapeseed oil in supercritical methanol under identical conditions (d), (e), (f)

formed when only methanol was used for synthesis. On the other hand, in the case of ZnO nanoparticles formed during transesterification, their TEM images showed nanosized primary particles coalescing at the edges of dense nanoparticle aggregates, indicating that the FAME molecules were chemically attached to the surfaces of the primary ZnO nanoparticles, resulting in steric hindrance. The smaller size of the nanoparticles formed during transesterification indicated that the continuous production of such nanoparticles could be scaled up with ease. In a scaled up continuous process, the coil-type tubular reactor would be less likely to be subject to plugging [17].

FT-IR spectroscopy was performed on both the various biodiesels and the ZnO nanoparticles formed under different process conditions. Figure 3.6 shows the FT-IR spectra of the biodiesel synthesized using only methanol (a), that synthesized using methanol and zinc nitrate (b), and pure rapeseed oil (c). The characteristic peaks noticed in the spectra were those related to the methyl group (–CH_3–) at 3000 cm^{-1}; methylene group (–CH_2–) at 2920 cm^{-1} and 2855 cm^{-1}; carbonyl group (–C=O) at 1742 cm^{-1}; and alkenyl group (–C=C–) at 1460 cm^{-1}. All three spectra had identical peaks. This shows that the biodiesel made from rapeseed oil was pure and that there was no change in the molecular structure of the FAMEs. The FT-IR spectrum of the ZnO nanoparticles formed in neat methanol and that of the ZnO nanoparticles formed during the biodiesel synthesis process are shown in Figures 3.7(a) and 3.7(b), respectively. The ZnO nanoparticles formed in neat methanol did not have any distinct characteristic peaks, except for a very broad peak attributable to the hydroxyl group (–OH). However, the ZnO nanoparticles formed during the biodiesel synthesis process had a broad –OH peak over the wavenumber range of 3000–3700 cm^{-1}. This was in addition to the characteristic FAME-related peaks shown in Figure 3.6. It has been previously reported that a broad –OH peak exists in the spectrum of ZnO nanoparticles formed during the synthesis of zinc oxide in supercritical methanol using fatty acids as surface modifiers [35]. In the case of the ZnO nanoparticles formed during biodiesel synthesis (Figure 3.7(b)), the presence of the peak related to the carboxylate group (–COO) at 1565 cm^{-1} confirmed that the FAME molecules had chemically bonded to the surfaces of the ZnO

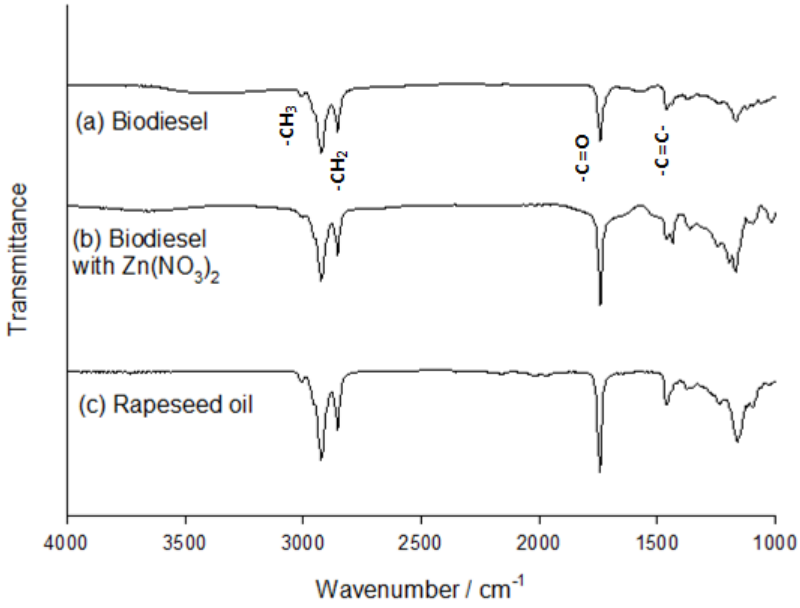

Figure 3.6. FT-IR spectra of the biodiesels synthesized using supercritical methanol (a) without zinc nitrate and (b) with zinc nitrate. (c) is the spectrum of neat rapeseed oil

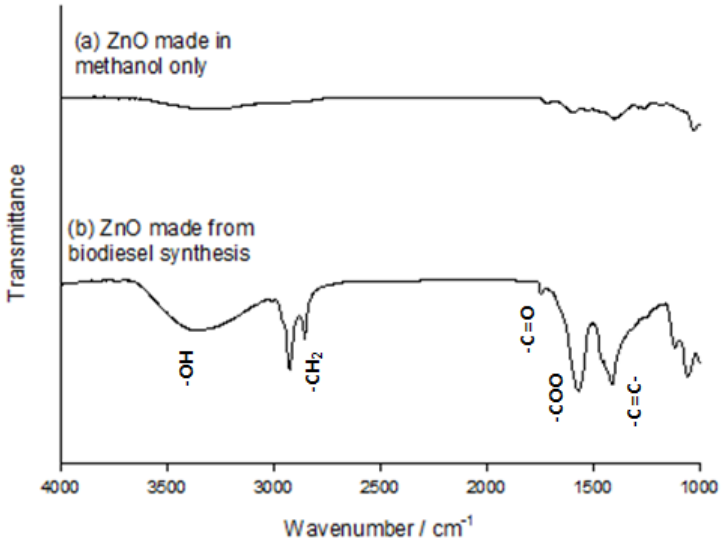

Figure 3.7. FT-IR spectra of the ZnO nanoparticles (a) synthesized in neat supercritical methanol and (b) synthesized during the transesterification of rapeseed oil

nanoparticles.

3.3.3 Experiments on various metals and metal oxides: A test on other metal precursors

Aside from zinc nitrate, other metal nitrates such as nickel, cobalt, cerium and iron nitrates were examined for their catalytic activity and metal compound formation. Table 3.2 is the summary of reaction temperature, time, FAME yield, type of metal precursor, and the particles formed. Various types of nanoparticles such as metal, metal hydroxide, metal oxide, etc. were formed depending on the metal atom and the process temperature. The nitrate ion of the metal nitrate is released as nitric acid which exists in glycerol, the more hydrophilic part of the product mixture. Details of the precursors used, process operating conditions, and the results are discussed below.

Zinc, cerium, iron, nickel and cobalt nitrate were tested for their catalytic activity and metal compound formation as a nanoparticle product. The results are shown in Figure 3.8, where the five different metal nitrates were tested at three different temperatures, 250, 300 and 350 °C. Zinc and cobalt nitrates yielded the highest FAME content, 96.88 % and 86.44 % respectively, at a relatively mild condition of 250 °C. FAME yields when cerium and iron nitrates were used were relatively low at 63.02 % and 52.67 % respectively for the same temperature. Nickel nitrate appeared to have almost no catalytic activity at 250 °C since its FAME contents were identical to uncatalyzed transesterification. With the exception of zinc nitrate, all the metal nitrates showed increased catalytic activity when the temperature was increased from 250 °C to 300 °C. At 350 °C, uncatalyzed transesterification yielded the highest FAME content which is due to thermal degradation of the FAMEs when the reaction was catalyzed. The overall result demonstrated that zinc nitrate was the best catalyst for lowering operating temperature. A simple ranking of the five metal nitrates for transesterification purpose can be stated as following: Zn > Co > Ce > Fe > Ni.

Nitrates of zinc, cerium and iron were oxidized to zinc oxide, cerium oxide, and iron oxide respectively, when they were introduced in the batch reactor along with rapeseed oil and methanol for reaction. Knowing that crystalline ZnO nanoparticles are synthesized during transesterification at 300 °C [36], reaction time was varied between 1 to 20 minutes to understand

No.	Temp.	Metal precursor	Reaction time	Particle phase	Particle morphology	FAME yield
	(°C)		(min)			(%)
1	250	N/A	1	N/A	N/A	1.09
2	250		5			1.61
3	250		10			18.83
4	250		20			28.60
5	300		1			3.91
6	300		5			14.94
7	300		10			26.55
8	300		20			92.73
9	350		1			70.81
10	350		5			92.99
11	350		10			91.46
12	350		20			88.95
13	400		1			90.61
14	400		5			77.47
15	400		10			64.02
16	400		20			52.99
17	300	$Zn(NO_3)_2$	1	Amorphous	Irregular spherical aggregates	91.84
18	300		5	ZnO		92.95
19	300		10	ZnO		93.92
20	300		20	ZnO		92.63
21	250		10	Amorphous		96.88
22	300		10	ZnO		93.92
23	350		10	ZnO		88.79
24	250	$Ce(NO_3)_3$	10	CeO_2	Irregular aggregates	63.02
25	300		10	CeO_2		92.08
26	350		10	CeO_2		86.83
27	250	$Fe(NO_3)_3$	10	Amorphous	Irregular aggregates	52.67
28	300		10	Fe_3O_4		81.40
29	350		10	Fe_3O_4		83.46
30	250	$Ni(NO_3)_2$	10	$Ni(OH)_2$ + $Ni_3(NO_3)_2(OH)_4$	Petal-like	18.79
31	300		10	$Ni(OH)_2$		63.31
32	350		10	Ni		86.66
33	400		10	Ni		N/A
34	250	$Co(NO_3)_2$	10	$Co(CH_3O)_x(NO_3)_y$	Petal-like	86.44
35	300		10	$Co(CH_3O)_x(NO_3)_y$		89.34
36	350		10	$Co(CH_3O)_x(NO_3)_y$ + Co		87.08
37	400		10	Co		N/A

Table 3.2. A summary of process operating conditions, FAME yields, and resulting particle characteristics

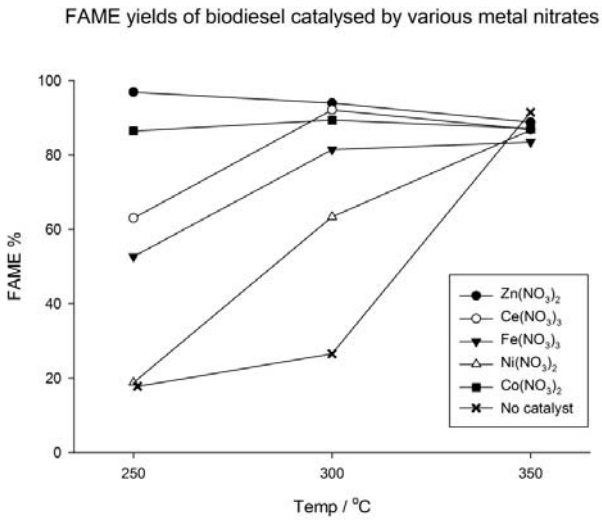

Figure 3.8. FAME yields of biodiesel synthesized using various metal nitrates at different temperatures. (Methanol to oil ratio = 40, pressure = 350 bar, time = 10 min)

the minimum reaction time necessary for crystalline metal compound formation. Results are shown in Figure 3.9(a) where 1 minute reaction time yielded amorphous ZnO nanoparticles and the crystallinity gradually increased along with increased reaction time. At 300 °C, a minimum of 10 minutes were required to obtain distinguishable XRD peaks which could be well indexed to JCPDS Card No. 79-0208. Three sets of temperatures (250, 300 and 350 °C) were also tested for ZnO synthesis, shown in Figure 3.9(b). ZnO nanoparticles showed a clear crystallinity from 300 °C. The same sets of temperatures and reaction time were applied to cerium nitrate and iron nitrate, shown in Figure 3.10(a) and 3.10(b) respectively. XRD patterns of cerium oxide (CeO_2) nanoparticles showed little increase in intensity with temperature increase. Only plane (111) was noticeable when indexed with JCDPS Card No. 34-0394, the other peaks were not large enough for indexing. This low crystallinity is thought to be caused by two factors, one is the existence of rapeseed oil during crystallization which hinders mass transfer of cerium ions in the methanol medium and the other is due to the low temperature of synthesis. On the other hand, iron oxide (Fe_3O_4, magnetite) showed identical crystallinity characteristics with ZnO when temperature was increased. Whilst amorphous phase was observed at 250 °C, particles synthesized at 300 °C and 350 °C displayed XRD patterns that were in good match with JCPDS Card No. 88-0315. Magnetite (Fe_3O_4) was synthesized instead of hematite (Fe_2O_3) due to the reducing environment of supercritical methanol [30]. This is the quality that distinguishes alcohol from other common solvents such as water, the ability to provide a reducing atmosphere for materials synthesis.

SEM images were taken to investigate the morphologies of the synthesized metal compounds, shown in Figure 3.11. The synthesis conditions were 300 °C, 350 bar and 10 minutes. Figure 3.11 (a) shows ZnO nanoparticles which are identical to the previously reported morphology [36]. CeO_2 showed irregular shape and size with dense flocculation (Figure 3.11(b)). FT-IR spectra were analyzed to study the surface characteristics of the nanoparticles. The spectra shown in Figure 3.12(a-c) are from ZnO, CeO_2 and Fe_3O_4 respectively, formed at 300 °C, 350 bar and 10 minutes. Bands in the 2830 – 2970 cm^{-1} region are assigned to methylene groups' C–H stretching vibration which comes from the aliphatic carbon chain of the fatty acids. The peak at 1565 cm^{-1}

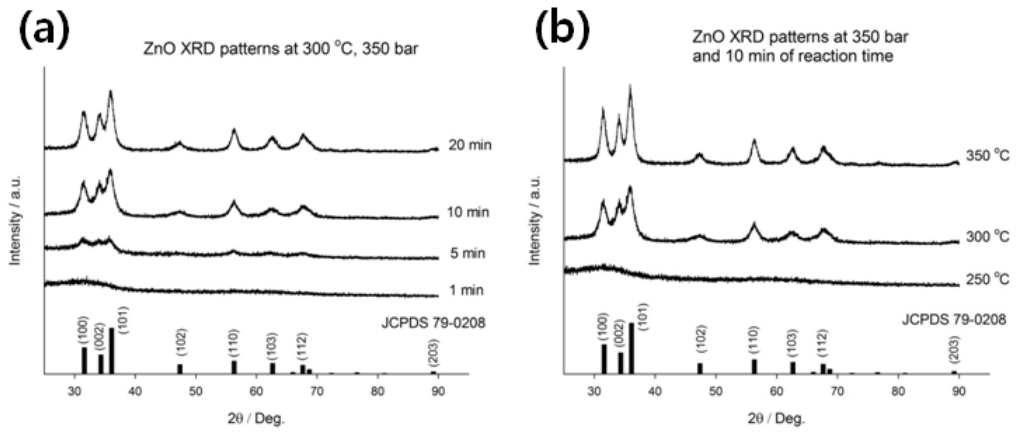

Figure 3.9. XRD patterns of ZnO (a) synthesized at 300 °C and 350 bar with time variation, and (b) synthesized at 350 bar and 10 minute reaction time with temperature variation

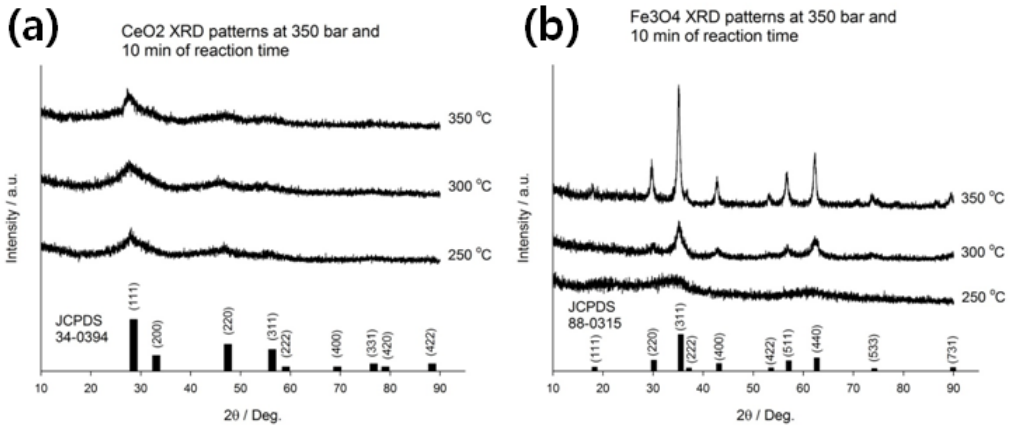

Figure 3.10. XRD patterns of (a) CeO_2 and (b) Fe_3O_4 with change in temperature (Pressure = 350 bar, time = 10 min)

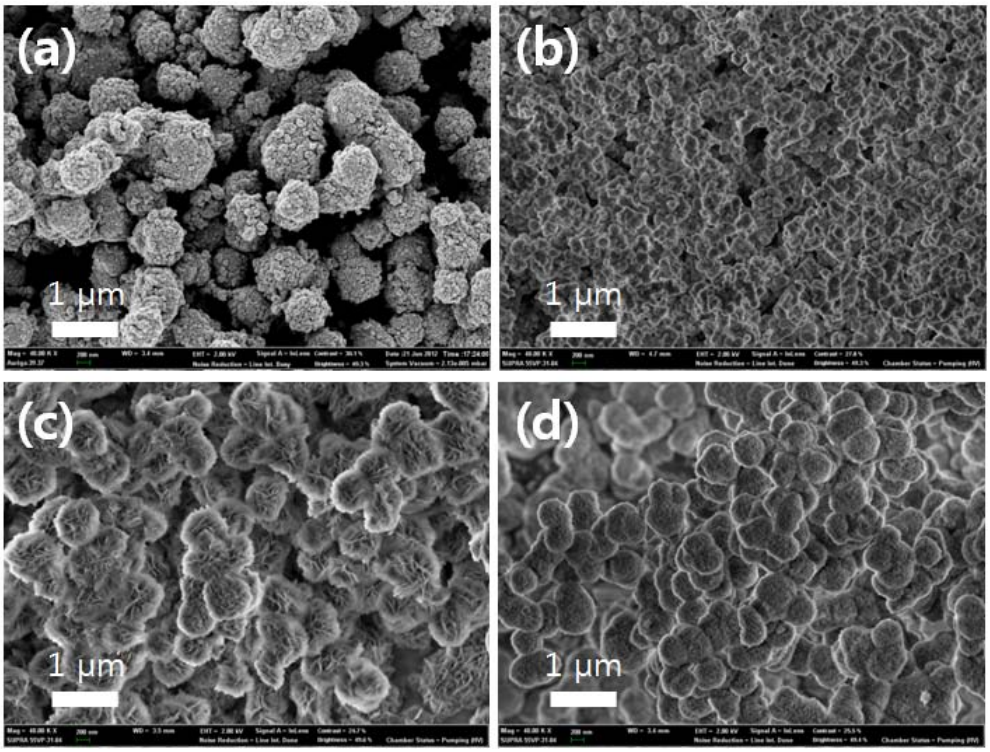

Figure 3.11. SEM images of (a) ZnO, (b) CeO_2, (c) $Ni(OH)_2$, and (d) $Co(OH)_2$ (Temperature = 300 °C, Pressure = 350 bar, time = 10 min)

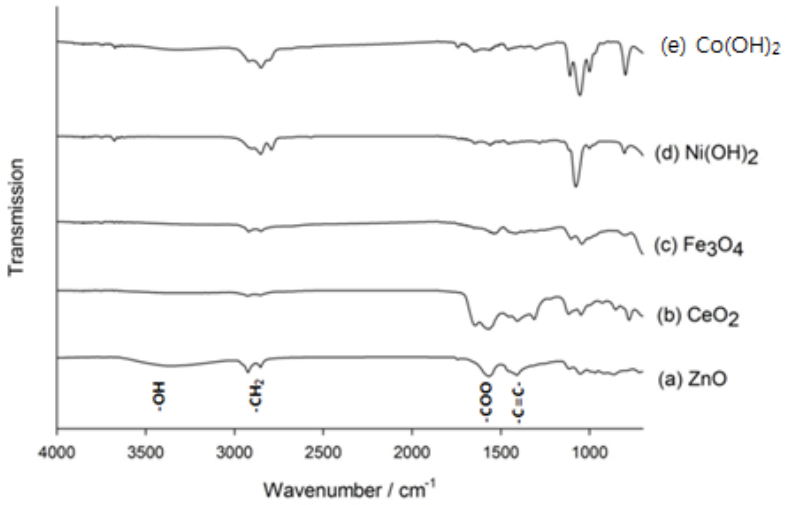

Figure 3.12. FT-IR spectra of (a) ZnO, (b) CeO_2, (c) Fe_3O_4, (d) $Ni(OH)_2$ and (e) $Co(CH_3O)_x,(NO_3)_y$ (Temperature = 300 °C, Pressure = 350 bar, time = 10 min)

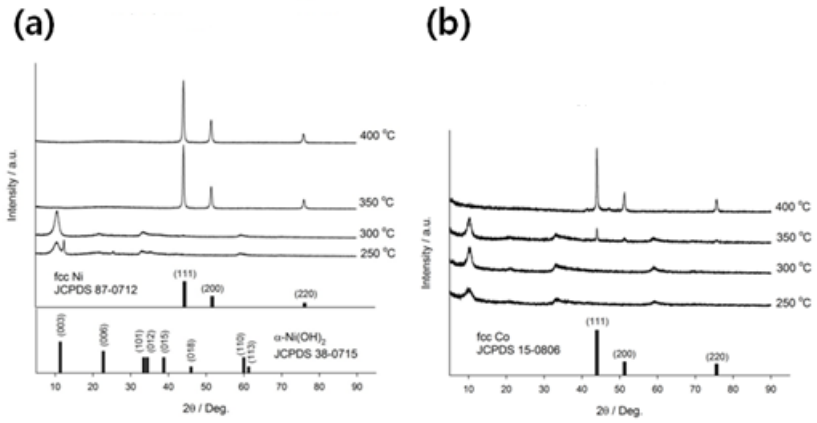

Figure 3.13. XRD patterns of (a) Ni and $Ni(OH)_2$ and (b) Co and $Co(OH)_2$ with change in temperature (Pressure = 350 bar, time = 10 min)

corresponds to the stretching frequency of the carboxylate group (–COO) indicating that the FAME molecules are chemically bonded to the surfaces of metal oxides [10]. Nitrates of nickel and cobalt yielded somewhat different products in contrast to the nitrates of zinc, cerium and iron. Figure 3.13 shows combined XRD patterns of (a) nickel and nickel hydroxide, and (b) cobalt and cobalt hydroxide. Nickel nitrate treated at 250 and 300 °C turned into α-$Ni(OH)_2$, which fit well with JCPDS Card No. 38-0715. The impurity peaks at 12.6° and 25.7° in the patterns of α-$Ni(OH)_2$ made at 250 °C are peaks from a reaction intermediate, nickel nitrate hydroxide ($Ni_3(NO_3)_2(OH)_4$), JCPDS Card No. 22-0752. Pure alpha phase nickel hydroxide was produced by increasing the temperature to 300 °C. Raising the temperature further to 350 and 400 °C resulted in the synthesis of face centered cubic (fcc) Ni nanoparticles, which were perfectly indexed with JCPDS Card No. 87-0712 [37]. The outcomes of cobalt compounds were similar to nickel compounds. The XRD patterns of cobalt compounds synthesized at 250 and 300 °C were cobalt hydroxide. When the temperature was increased to 350 °C, new peaks appeared at 43.9°, 51.1° and 75.6° which represent (111), (200) and (220) planes of fcc cobalt, respectively. Increasing the temperature further to 400 °C resulted in the formation of pure fcc cobalt that was well-indexed with JCPDS Card No. 15-0806.

Morphologies of nickel hydroxide and cobalt methoxynitrate were checked with SEM (Figure 3.11 (c) and (d)). Both materials had irregular submicron size with petal-like shape. FT-IR spectra shown in Figure 3.12 (d) and (e) showed identical characteristics with that of the aforementioned metal oxides. The characteristic peaks of alkyl chains and carboxylate groups showed that the fatty acids were chemically bonded with the aliphatic chain pointing outward of the nanoparticles.

The synthetic products of nickel and cobalt were gradually reduced with increase in operating temperature to finally obtain pure metal nanoparticles at either 350 °C or 400 °C. This phenomenon is possible because alcohols in supercritical state can reduce metal ions to a lower valence state [5, 29, 37]. From this study, it can be stated that solvothermal synthesis using near-critical alcohols allows the production of metals, metal hydroxides and various other metal compounds that may not be produced in hydrothermal conditions.

3.3.4 Proposed formation mechanisms of metals, metal hydroxides, and metal oxides in supercritical methanol

The ramp up time to reach the supercritical conditions is two and a half minutes in our batch reactor and molten salt bath system. During ramp up, the metal nitrates ($M(NO_3)_n$) undergo alcoholysis to become metal methoxides ($M(OCH_3)_n$). This metal methoxide is subsequently hydrolyzed to a metal oxide ($MO_{n/2}$). There are two possible sources of hydrolysis; from the hydroxyl ions of methanol [13] and from the water that came with metal nitrate precursor, i.e. zinc nitrate hexahydrate ($Zn(NO_3)_2 \cdot 6H_2O$). The metal oxide is reduced to metal by reacting with the hydrogen provided by methanol at high temperature. Figure 3.14 represents the proposed mechanisms of metal oxide formation and metal reduction in supercritical methanol.

Under the identical supercritical methanol conditions, zinc and cerium nitrates were oxidized, whereas nickel and cobalt nitrates were reduced. This difference may be explained with the standard reduction potentials of the metal ions provided in literature (Table 3.3) [38]. The larger the standard reduction potential, the more likely they are to be reduced. Iron nitrate has the largest reduction potential (+0.771 V) out of all five metals, therefore Fe_3O_4 was made instead of Fe_2O_3. Nickel and cobalt ions were in the -0.25 V to -0.29 V range which were higher than that of zinc or cerium ions having -0.762 V and -2.34 V, respectively.

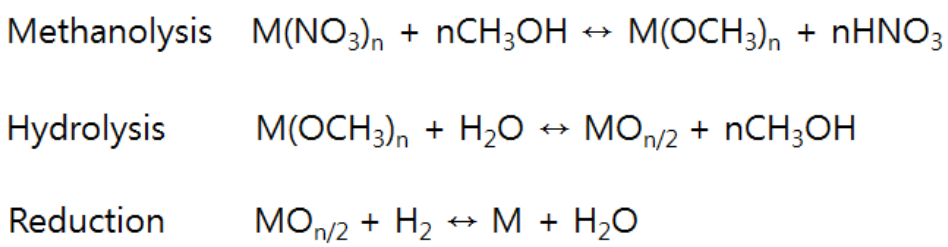

Figure 3.14. Proposed mechanisms of metal oxide formation and metal reduction in supercritical methanol

Couple	E° / V
$Fe^{3+} + e^- \rightarrow Fe^{2+}$	+ 0.771
$Ni^{2+} + 2e^- \rightarrow Ni$	- 0.257
$Co^{2+} + 2e^- \rightarrow Co$	- 0.282
$Zn^{2+} + 2e^- \rightarrow Zn$	- 0.762
$Ce^{3+} + 3e^- \rightarrow Ce$	- 2.34

Table 3.3. Standard reduction potentials at 25 °C (From acidic solutions) [38]

3.4 Summary

Various metal (Zn, Ce, Fe, Ni, Co) nitrates were used as catalysts during the transesterification of rapeseed oil in supercritical methanol to obtain biodiesel, glycerol and metal compounds as products. Zinc nitrate was the best catalyst out of the five different metal nitrates with 96.88 wt% FAME yield at 250 °C, 350 bar and 10 minutes. Also at 300 °C, the FAME yields were all above 91 wt% regardless of reaction time which was varied between 1 – 20 min. The use of metal nitrates as catalysts for transesterification reactions under supercritical methanol conditions has two major advantages. First is the lowering of operational temperature and time which has the potential of reducing utility costs for large scale production. Second is the synthesis of metal compounds such as metal, metal hydroxide, metal oxide, etc. Methanol has two functions in our system; as a reaction medium and as a reducing agent. The reduced nanoparticles take various forms depending on the process temperature and are prepared in a short period of reaction time (10 – 20 min).

Chapter Four

Hydrothermal synthesis of metal nanoparticles using glycerol as a reducing agent

Chapter 4. Hydrothermal synthesis of metal nanoparticles using glycerol as a reducing agent

4.1 Introduction

Synthesis methods of metal nanoparticles have been under research for decades since they are used in various fields of industry such as catalysis, ceramics, coatings, magnetic materials, etc. Commonly known solution methods for synthesizing metal nanoparticles are polyol process [39], micro-emulsion [40], chemical reduction [41], solvothermal [5, 29], and inverse micelle [42]. Each methods have their own advantages and disadvantages. The common disadvantages are the use of toxic reagents, requiring an inert atmosphere, and the need for organic waste treatment. As an alternative, hydrothermal crystallization of metal oxides was first introduced by Adschiri et al. [6] which heats up aqueous acidified metal salt solution to a supercritical state of 400 ˚C and 35 MPa. Despite the high temperature and pressure, the supercritical water (SCW) method allows rapid and simple synthesis of pure metal oxides which is an environmentally friendly process. Water is cheap, abundant, environmentally benign, and is a well-known oxidizing agent as well as a solvent. In spite of the water's strong oxidizing nature, there have been several attempts to synthesize metals using SCW with formic acid as a reducing agent. Sue et al. produced nickel fine particles [43], Ohara et al. and Seong et al. have successfully synthesized cobalt nanoparticles [44, 45], and Arita et al. attempted to synthesize iron nanoparticles [46], all in the presence of SCW and formic acid.

Supercritical alcohol was also found to be a superb reductive medium. Kim et al. synthesized copper, nickel and silver using supercritical methanol at 400 ˚C without any reducing agents or stabilizers [5]. The supercritical alcohol was not only the reaction solvent but also a reducing agent. Supercritical methanol was also used for synthesizing cobalt nanoparticles [29] and magnetite nanoparticles [30]. Synthesis of metals or metal oxides using supercritical alcohols have the advantage of not using any reductants which allows simpler production process and

product recovery.

In this chapter, we examined the hydrothermal reduction of metals and metal oxides using SCW as a reaction medium and glycerol as a reducing agent. Silver, copper, nickel, cobalt, iron and manganese nitrates were tested for their reduction. Glycerol differs from other reductants in many ways; it is readily available, environmentally benign, odorless, safe upon skin contact, and does not require a glovebox for formulation. Reducing agents themselves become oxidized during reaction. Glycerol can be oxidized into many products such as glyceraldehyde, glyceric acid, dihydroxy acetone, hydroxypyruvinic aldehyde, etc [47]. Glycerol treated in SCW can also dehydrate to form acrolein. Therefore, various glycerol-derived chemicals can be made simultaneously.

4.2 Experimental

4.2.1 Materials

The metal precursors were nickel (II) nitrate (Hayashi Pure Chemical), copper (II) nitrate (Shinyo Pure Chemical), silver (I) nitrate (Sigma-Aldrich), cobalt (II) nitrate (Junsei Chemical), iron (III) nitrate (Sigma-Aldrich) and Manganese (II) nitrate (Kanto Chemical), which were all used as received. Glycerol was obtained from Sigma-Aldrich and water was deionized using Millipore Milli-Q Advantage A10 apparatus.

4.2.2 Experimental procedure

The hydrothermal synthesis of metal nanoparticles was carried out in a stainless steel (SUS316) reactor with an inner volume of 23 ml. A thermostat-monitored salt bath system (Salt bath content: $NaNO_3 – KNO_3 – Ca(NO_3)_2$ = 46:24:30) was used to heat up the reactor to the desired reaction temperature. For a typical synthesis, an appropriate amount of 0.1 M metal nitrate precursor solution was placed in the reactor so that the pressure would be 300 bar at 400 ˚C. Water density data from NIST Chemistry Webbook [http://webbook.nist.gov/chemistry/] was used for pressure

calculations. The reducing agent glycerol was added to the reactor according to the prescribed mole ratio of glycerol to metal precursor which was 5 to 15. The reactor loaded with metal salt solution and glycerol was tightly sealed and put into the salt bath for 10 minutes with constant shaking. After 10 minutes, the reaction inside the reactor was terminated by rapidly quenching the reactor in a cool water bath. The resulting powders were isolated and washed three times with water to remove organic residues. The washed powders were dried in a vacuum oven at 80 ˚C for 24 hours.

4.2.3 Characterization

The hydrothermally synthesized nanoparticles were analyzed using X-ray diffraction (XRD; Rigaku D/Max-3C diffractometer with Cu Kα radiation) and scanning electron microscopy (SEM; Carl Zeiss Auriga). XRD patterns confirmed the phase and purity of the product nanoparticles, whether they were uncharged metals, reduced metal oxides or ordinary metal oxides. SEM images were taken to check the particle size and shape.

4.3 Results and discussion

4.3.1 Glycerol as a reducing agent in hydrothermal synthesis of metals (Ag, Cu, Ni)

Figure 4.1 shows the XRD patterns of silver, copper oxide, and copper made by hydrothermal synthesis using SCW at 400 ˚C and 300 bar. XRD patterns of silver oxide (Ag_2O) were not available because silver nitrate ($AgNO_3$) reacted at 400 ˚C had thermally degraded and no powders were obtained for physical study. However, when glycerol was used as a reductant, pure silver particles were obtained as shown in Figure 4.1(a). The mole ratio of glycerol to metal precursor was 5 for both silver and copper synthesis. Hydrothermal treatment of copper nitrate at 400 ˚C resulted in the formation of copper (II) oxide (Figure 4.1(b)). In contrast, when glycerol was used as a reductant, pure copper particles were formed, shown in Figure 4.1(c). Figure 4.2 shows the synthesis of nickel oxide and nickel by varying the amount of glycerol. Reduction of

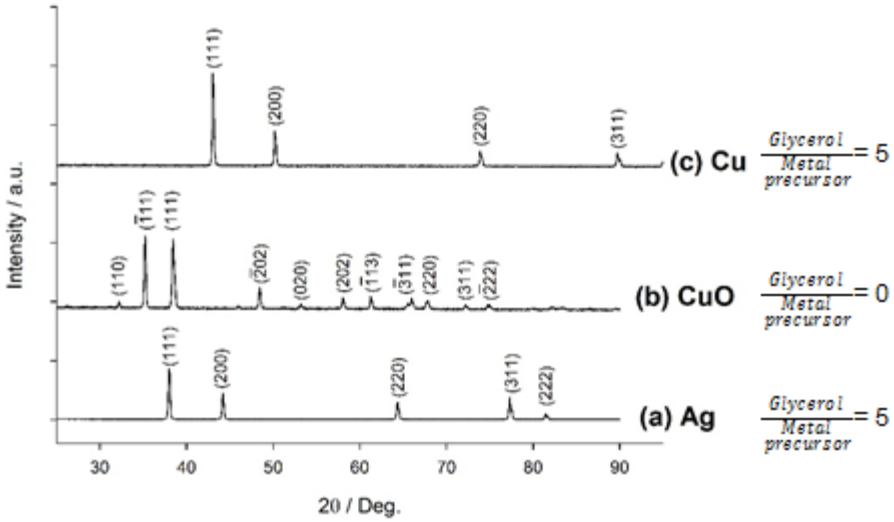

Figure 4.1. XRD patterns of (a) Ag, (b) CuO, and (c) Cu synthesized using SCW at 400 ˚C. Mole ratio of glycerol to metal precursor was 5 for Ag and Cu synthesis

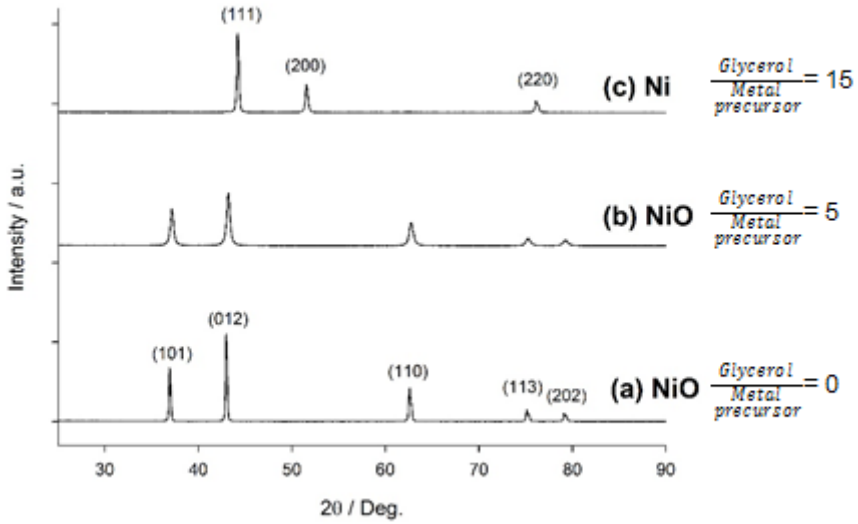

Figure 4.2. XRD patterns of (a) NiO, (b) NiO and (c) Ni synthesized using SCW at 400 ˚C. Mole ratio of glycerol to metal precursor was (a) 0, (b) 5, and (c) 15

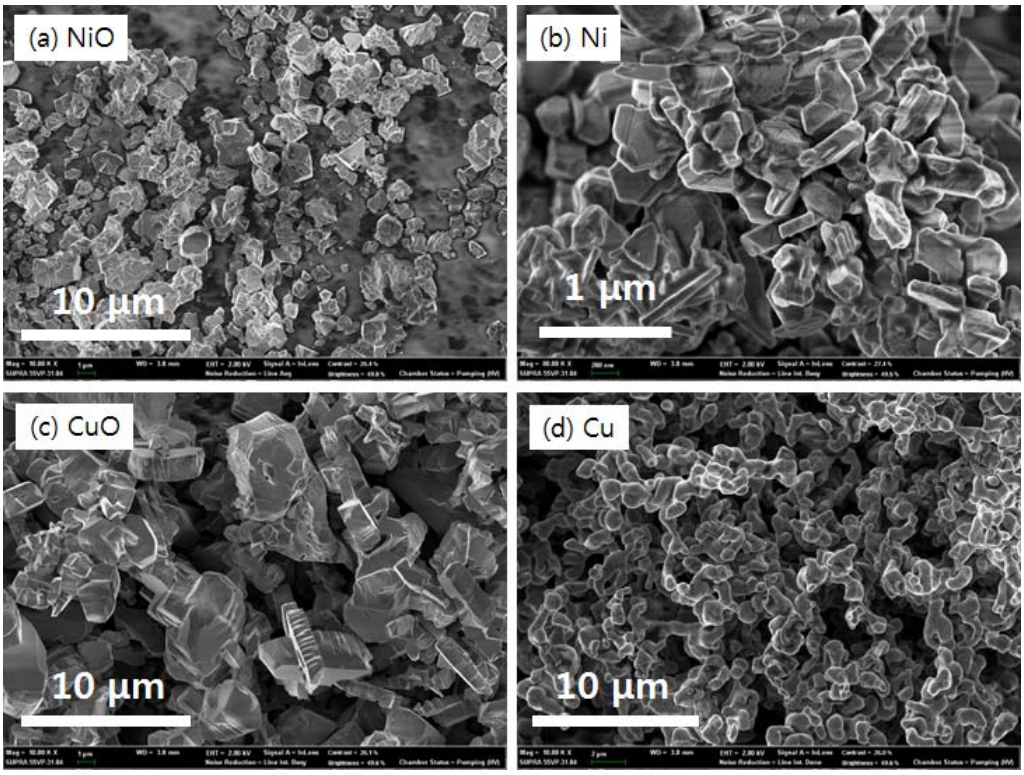

Figure 4.3. SEM images nanoparticles synthesized in SCW at 400 ˚C: (a) NiO, (b) Ni, (c) CuO, and (d) Cu

nickel was slightly more demanding, glycerol to metal precursor mole ratio of 5 wasn't enough for reduction (Figure 4.2(b)) and 15 mole ratio was required to synthesize pure Ni particles (Figure 4.2(c)). The SEM images of metal oxides and metals are shown in Figure 4.3. NiO particles had irregular shape with a broad size distribution of 100 – 3,000 nm. Ni particles also had irregular shape with smaller size and a size distribution of 100 – 1,000 nm. CuO and Cu were similar to NiO and Ni in terms of particle morphology and size, the copper oxide particles were relatively large in micron range compared to copper, which were submicron-sized aggregates.

4.3.2 Glycerol as an anti-oxidant in hydrothermal synthesis of metal oxides (CoO, Fe_3O_4, MnO)

Cobalt, iron and manganese nitrates were not fully reduced to zero-valent metals by hydrothermal treatment at 400 ˚C with glycerol. First, cobalt nitrate was treated with SCW at 400 ˚C with and without glycerol. A simple hydrothermal synthesis without any additives yielded Co_3O_4, cobalt (II, III) oxide, shown in Figure 4.4(a). When glycerol was added at a mole ratio of either 5 or 15, only CoO (cobalt (II) oxide) was formed (Figure 4.4(b) and 4.4(c)). The reducing agent glycerol behaved as an antioxidant in this case by preventing further oxidation of CoO into Co_3O_4. The same phenomenon was observed for the oxides of iron and manganese. Figure 4.5(a) shows the XRD patterns of Fe_2O_3 (hematite, iron (III) oxide) made by reacting iron nitrate in SCW. When 5 mole ratio of glycerol was added into the reactor together with iron nitrate, pure Fe_3O_4 (magnetite, iron (II,III) oxide) were acquired, shown in Figure 4.5(b). Figure 4.6 shows the identical case for manganese oxide formation. Hydrothermal synthesis at 400 ˚C without any additives resulted in pure MnO_2 (manganese (IV) oxide) formation (Figure 4.6(a)). A mixture of MnO (manganese (II) oxide) and $MnCO_3$ (manganese (II) carbonate) was made when 5 mole ratio of glycerol was added, as shown in Figure 4.6(b). $MnCO_3$ is an intermediate of MnO, where the source of carbon for carbonate formation is supplied by glycerol. MnO is formed as a result of $MnCO_3$ thermal decomposition which releases MnO and CO_2. Having a reductive intermediate $MnCO_3$ in the product indicates that the reduction process was still on going when the reactor was quenched to terminate the reaction. To gain a single phase MnO, increase in either reaction temperature or

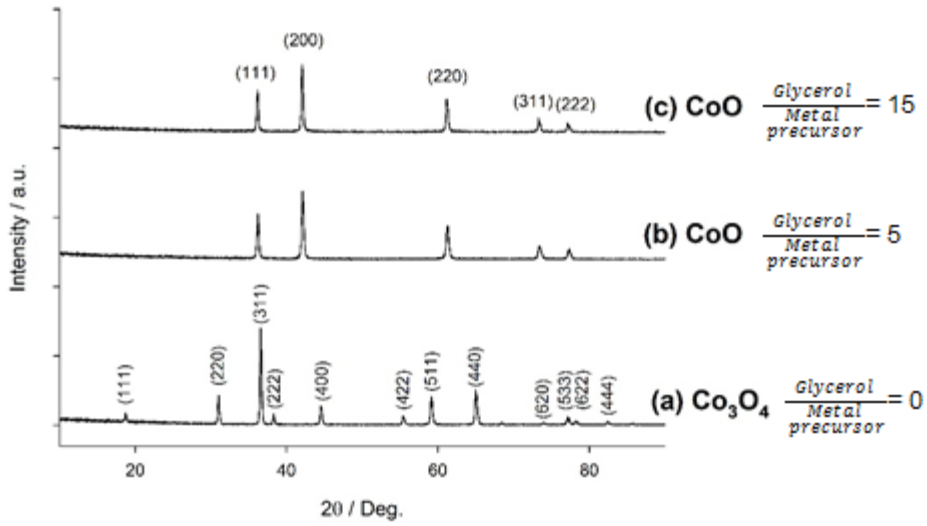

Figure 4.4. XRD patterns of (a) Co_3O_4, (b) CoO, and (c) CoO synthesized using SCW at 400 ˚C. Mole ratio of glycerol to metal precursor was (a) 0, (b) 5, and (c) 15

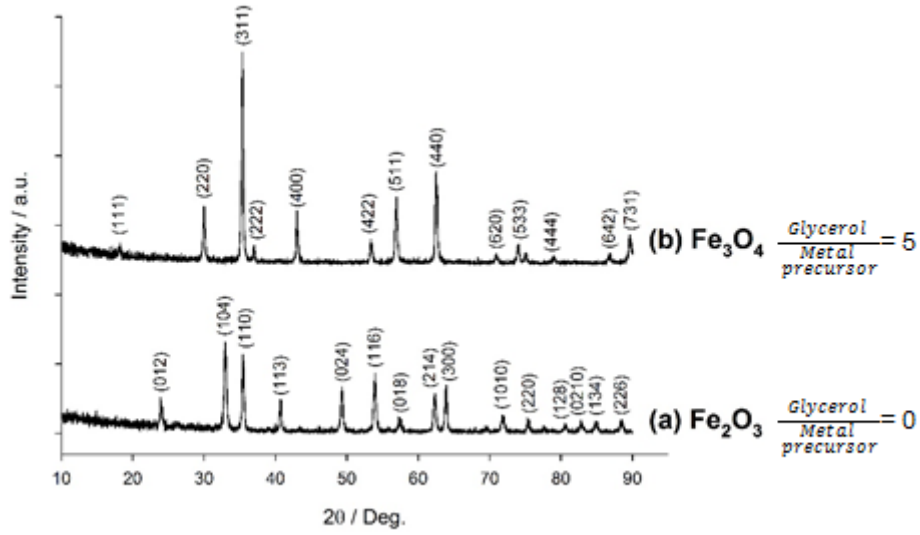

Figure 4.5. XRD patterns of (a) Fe_2O_3 and (b) Fe_3O_4 synthesized using SCW at 400 ˚C. Mole ratio of glycerol to metal precursor was (a) 0 and (b) 5

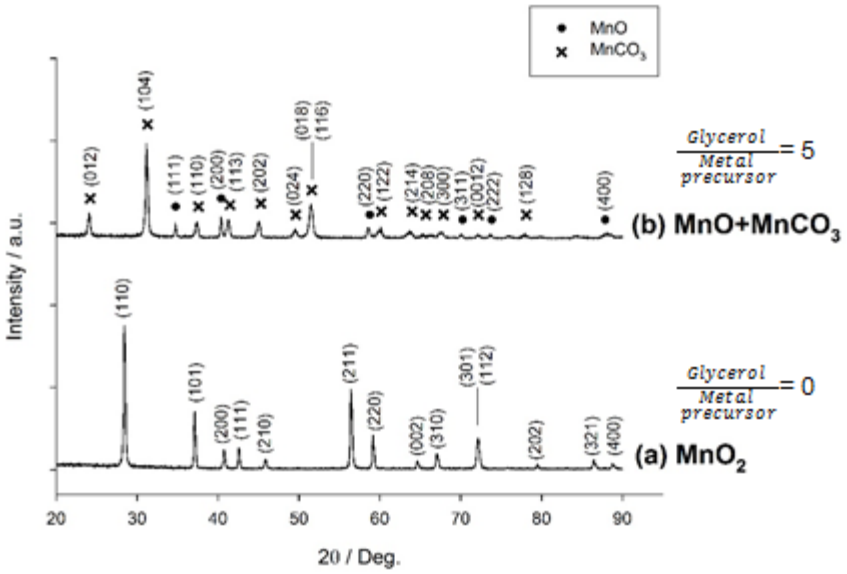

Figure 4.6. XRD patterns of (a) MnO_2 and (b) MnO + $MnCO_3$ synthesized using SCW at 400 ˚C. Mole ratio of glycerol to metal precursor was (a) 0 and (b) 5

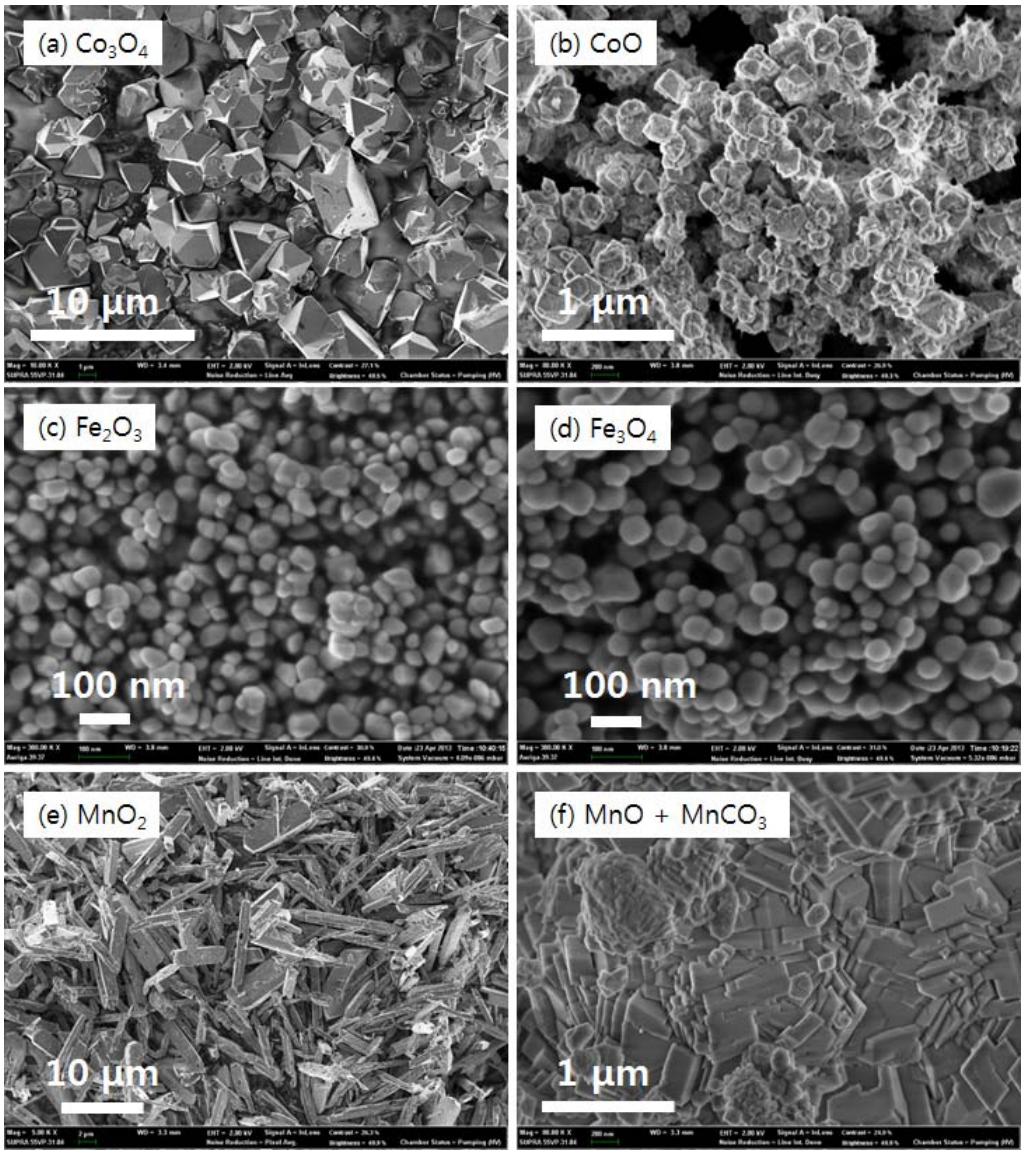

Figure 4.7. SEM images of nanoparticles synthesized in SCW at 400 ˚C. (a) Co_3O_4, (b) CoO, (c) Fe_2O_3, (d) Fe_3O_4, (e) MnO_2 and (f) MnO + $MnCO_3$

time is required to allow complete thermal decomposition of $MnCO_3$. Figure 4.7 shows the SEM images of the metal oxides. Co_3O_4 had an octahedral shape with 1 – 5 μm in size whereas, CoO was much smaller in 20 – 200 nm range, shown in Figure 4.7(a) and 4.7(b), respectively. Fe_2O_3 (Figure 4.7(c)) and Fe_3O_4 (Figure 4.7(d)) were relatively identical in size and shape which were 5 – 20 nm range. MnO_2 had a rod shape in the range of 2 – 20 μm whereas mixture of MnO + $MnCO_3$ was plate-like with sub-micron size (Figure 4.7(e) and 4.7(f)).

4.3.3 Difference in reduction potentials of elements

Silver and copper were easily reduced to metals with 5 mole ratio of glycerol whereas, nickel required 15 mole ratio of glycerol for complete reduction. Cobalt, iron and manganese were not completely reduced to zero-valent metals, however were reduced into partially reduced (or oxidized) metal oxides. The reduction tendency of the elements tested in this study are illustrated in Figure 4.8. Such difference in reduction tendency of elements can be explained using standard reduction potentials listed in Table 4.1 [38]. A reduction potential is a measure of the likeliness of an element to be reduced, thus an element having more positive potential is more likely to be reduced. Reduction potential of nickel having -0.257 V was the redox borderline which explains why cobalt and manganese nitrates were not reduced to zero-valent metals. Table 4.2 summarizes the overall results of metal and metal oxide formation from glycerol aided hydrothermal reduction.

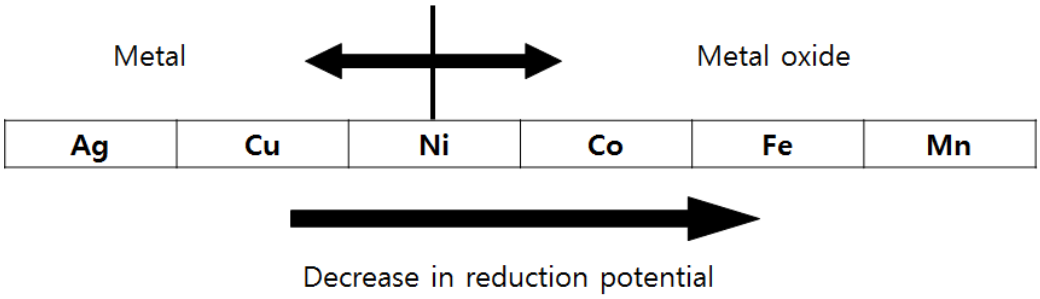

Figure 4.8. Reduction tendency of metals hydrothermally synthesized with glycerol

Couple	**E˚ / V**
$Ag^{+} + e^{-} \rightarrow Ag$	+ 0.799
$Fe^{3+} + e^{-} \rightarrow Fe^{2+}$	+ 0.771
$Cu^{2+} + 2e^{-} \rightarrow Cu$	+ 0.34
$Ni^{2+} + 2e^{-} \rightarrow Ni$	- 0.257
$Co^{2+} + 2e^{-} \rightarrow Co$	- 0.282
$Fe^{2+} + 2e^{-} \rightarrow Fe$	- 0.44
$Mn^{2+} + 2e^{-} \rightarrow Mn$	- 1.18

Table 4.1. Standard reduction potentials at 25 ˚C from acidic solutions

Type of metal precursor	Glycerol to metal precursor mole ratio	Metal product	Particle size / nm
$AgNO_3$	0	N/A	N/A
	5	Ag	2,000 – 5,000
$Cu(NO_3)_2 \cdot 3H_2O$	0	CuO	500 – 5,000
	5	Cu	200 – 2,000
$Ni(NO_3)_2 \cdot 6H_2O$	0	NiO	100 – 3,000
	5	NiO	100 – 3,000
	15	Ni	100 – 1,000
$Co(NO_3)_2 \cdot 6H_2O$	0	Co_3O_4	1,000 – 5,000
	5	CoO	20 – 200
	15	CoO	20 – 200
$Fe(NO_3)_3 \cdot 9H_2O$	0	Fe_2O_3	5 – 20
	5	Fe_3O_4	5 – 20
$Mn(NO_3)_2 \cdot 6H_2O$	0	MnO_2	2,000 – 20,000
	5	$MnO + MnCO_3$	50 - 500

Table 4.2. Summary of hydrothermal reduction of metal nitrates using SCW and glycerol

4.4 Summary

Various metal and metal oxide particles were synthesized in SCW at 400 ˚C and 300 bar with glycerol as a reducing agent. Silver, copper and nickel nitrates were completely reduced to zero-valent metals. On the other hand, cobalt, iron and manganese nitrates were partially reduced into low-valent metal oxides which indicate glycerol's role as an anti-oxidant. The prepared metals were generally smaller in size than their corresponding metal oxides. Glycerol is odorless, non-toxic, non-flammable, convenient to treat, environmentally friendly, and readily available compared to other reducing agents such as formic acid and hydrazine. The new glycerol hydrothermal reduction method is green as well as economic for scale-up production of various metals and metal oxides.

Chapter Five

Conclusion

Chapter 5. Conclusion

In this dissertation, the three major components:

1. Supercritical fluids (Water and Methanol)
2. Metal precursors (Metal Nitrates)
3. Vegetable oils (and their derivatives)

were used throughout the all chapters for the synthesis of metal and metal oxide nanoparticles. The major aim was to develop novel green engineering methods that were not attempted previously. There are many known techniques in producing nanoparticles such as the solid state method and solution chemistry method. The solid state method requires very high reaction temperature (800 – 1200 ˚C) and the solution chemistry method such as sol-gel use harsh organic solvents that cause waste disposal problems. The supercritical fluid utilized nanoparticle synthesis is a much more and environmentally benign option compared to the aforementioned methods. This thesis attempts to use the safest and the most environmentally friendly raw materials to achieve the goals that were previously reported by others such as Prof Adschiri's group in Tohoku University and Prof Saka's group in Kyoto Univeristy.

In chapter two, supercritical water, cerium nitrate, and vegetable oils (palm and soybean oil) were used. For the first time, vegetable oil was used in hydrothermal synthesis of cerium oxide nanoparticles. The aim was to use the readily available bioresources directly as a precursor of materials processing. As a result, well-dispersed cerium oxide nanocrystals were successfully synthesized with stable surface modification by various fatty acids. The surface modifying agents used by Adschiri group such as decanoic and hexanoic acids are high-purity reagents which are expensive due to the complex synthesis and purification steps involved during production. The

results imply that not only vegetable oils but also animal fats can be used for the same purpose which means cost reduction in raw materials as well as using the natural bioresources.

In chapter three, supercritical methanol, various metal nitrates, and vegetable oil (canola oil) were used for the simultaneous synthesis of metal products and biodiesel. The initial intention was simply switching the solvent from water to methanol which was one step forward from chapter two. However, biodiesel was also produced as a major product because of the transesterification between the triglycerides and methanol. The highest FAME yield was 96.88 wt% which was obtained at 250 ˚C, 350 ba, 10 min with 3 oil wt% loading of zinc nitrate. The simultaneously synthesized metal products were surface modified by the FAME molecules in-situ. This newly developed simultaneous synthesis process provides an economic advantage as it reduces operation temperature and time, and produces metal products as by-products.

In chapter four, supercritical water, various metal nitrates, and glycerol was used for hydrothermal reduction of metal nanoparticles at 400 ˚C and 300 bar for 10 minutes. Previously, formic acid or hydrazine were used as reducing agents by Adschiri group. Glycerol as a reducing agent was found to reduce silver, copper and nickel nitrates fully into zero-valent metals. Cobalt, iron and manganese nitrates were partially reduced to their low-valent metal oxides. Glycerol compared to formic acid or hydrazine is odorless, safe, easy to handle, and environmentally benign. The glycerol hydrothermal reduction method developed in this chapter is so far the greenest chemical reduction technique in terms of raw materials.

To conclude, three chapters in this dissertation were devoted in developing novel and green processes of synthesizing nanoparticles using supercritical fluids. The raw materials are all of low-cost, environmentally friendly, and is readily available in nature. The synthesis techniques developed within this thesis is expected to be applicable for all the metal atoms in the periodic table. Further study in the field may consist of test on other solvents apart from water and methanol as well as solvent mixtures. The effect of supercritical fluids' treatment on glycerol is another area of in depth research that needs attention. Various organic compounds are known to

be formed by reacting glycerol with supercritical fluids which are used as important precursors in the chemical industry.

References

[1] P.T. Anastas, W. J.C., Green Chemistry: Theory and Practice, in, Oxford University Press: New York, 1998.

[2] P.T. Anastas, J.B. Zimmerman, Peer Reviewed: Design Through the 12 Principles of Green Engineering, Environmental Science & Technology, 37 (2003) 94A-101A.

[3] T. Arai, T. Sako, Y. Takebayashi, Supercritical Fluids: Molecular Interactions, Physical Properties, and New Applications, in, Springer-Verlag Berlin Heidelberg, 2002.

[4] P. Kritzer, N. Boukis, E. Dinjus, Factors controlling corrosion in high-temperature aqueous solutions: a contribution to the dissociation and solubility data influencing corrosion processes, The Journal of Supercritical Fluids, 15 (1999) 205-227.

[5] J. Kim, D. Kim, B. Veriansyah, J. Won Kang, J.-D. Kim, Metal nanoparticle synthesis using supercritical alcohol, Materials Letters, 63 (2009) 1880-1882.

[6] T. Adschiri, K. Kanazawa, K. Arai, Rapid and Continuous Hydrothermal Crystallization of Metal Oxide Particles in Supercritical Water, Journal of the American Ceramic Society, 75 (1992) 1019-1022.

[7] M.H. Zuknik, N.A. Nik Norulaini, A.K. Mohd Omar, Supercritical carbon dioxide extraction of lycopene: A review, Journal of Food Engineering, 112 (2012) 253-262.

[8] A.G. Carr, R. Mammucari, N.R. Foster, A review of subcritical water as a solvent and its utilisation for the processing of hydrophobic organic compounds, Chemical Engineering Journal, 172 (2011) 1-17.

[9] O.J. Catchpole, J.B. Grey, N.B. Perry, E.J. Burgess, W.A. Redmond, N.G. Porter, Extraction of Chili, Black Pepper, and Ginger with Near-Critical CO2, Propane, and Dimethyl Ether: Analysis of the Extracts by Quantitative Nuclear Magnetic Resonance, Journal of Agricultural and Food Chemistry, 51 (2003) 4853-4860.

[10] J. Zhang, S. Ohara, M. Umetsu, T. Naka, Y. Hatakeyama, T. Adschiri, Colloidal Ceria Nanocrystals: A Tailor-Made Crystal Morphology in Supercritical Water, Advanced Materials, 19 (2007) 203-206.

[11] T. Arita, J. Yoo, T. Adschiri, Relation between the Solution-State Behavior of Self-Assembled Monolayers on Nanoparticles and Dispersion of Nanoparticles in Organic Solvents, The Journal of Physical Chemistry C, 115 (2011) 3899-3909.

[12] D. Rangappa, S. Ohara, T. Naka, A. Kondo, M. Ishii, T. Adschiri, Synthesis and organic modification of CoAl2O4 nanocrystals under supercritical water conditions, Journal of Materials Chemistry, 17 (2007) 4426-4429.

[13] T. Arita, K.-i. Moriya, T. Yoshimura, K. Minami, T. Naka, T. Adschiri, Dispersion of Phosphonic Acids Surface-Modified Titania Nanocrystals in Various Organic Solvents, Industrial & Engineering Chemistry Research, 49 (2010) 9815-9821.

[14] K.J. Klabunde, R. Richards, Nanoscale Materials in Chemistry 2nd Ed, Wiley, Hoboken, N.J., 2009.

[15] A. Bumajdad, J. Eastoe, A. Mathew, Cerium oxide nanoparticles prepared in self-assembled systems, Advances in Colloid and Interface Science, 147–148 (2009) 56-66.

[16] Y.-W. Lee, Design of Particles using Supercritical Fluids, HWAHAK KONGHAK, 41 (2003) 689-688.

[17] T. Adschiri, Y.-W. Lee, M. Goto, S. Takami, Green materials synthesis with supercritical water, Green Chemistry, 13 (2011) 1380-1390.

[18] A. Ahniyaz, Y. Sakamoto, L. Bergström, Tuning the Aspect Ratio of Ceria Nanorods and Nanodumbbells by a Face-Specific Growth and Dissolution Process, Crystal Growth & Design, 8 (2008) 1798-1800.

[19] T. Yu, J. Joo, Y.I. Park, T. Hyeon, Large-Scale Nonhydrolytic Sol–Gel Synthesis of Uniform-Sized Ceria Nanocrystals with Spherical, Wire, and Tadpole Shapes, Angewandte Chemie, 117 (2005) 7577-7580.

[20] T. Yu, B. Lim, Y. Xia, Aqueous-Phase Synthesis of Single-Crystal Ceria Nanosheets,

Angewandte Chemie International Edition, 49 (2010) 4484-4487.

[21] J.P. Cosgrove, J.G. Hayden, P.L. Robinson, PROCESS FOR MAKING HIGH-PURITY OLEIC ACID, in, 1993.

[22] Y.K. Hong, W.H. Hong, Biodiesel Production Technology and Its Fuel Properties, Korean Chem. Eng. Res., 45 (2007) 424-432.

[23] Y.G. Aronoff, B. Chen, G. Lu, C. Seto, J. Schwartz, S.L. Bernasek, Stabilization of Self-Assembled Monolayers of Carboxylic Acids on Native Oxides of Metals, Journal of the American Chemical Society, 119 (1997) 259-262.

[24] A.K. Singh, S.D. Fernando, Transesterification of Soybean Oil Using Heterogeneous Catalysts, Energy & Fuels, 22 (2008) 2067-2069.

[25] E.M. Shahid, Y. Jamal, Production of biodiesel: A technical review, Renewable and Sustainable Energy Reviews, 15 (2011) 4732-4745.

[26] J.-S. Lee, S. Saka, Biodiesel production by heterogeneous catalysts and supercritical technologies, Bioresource Technology, 101 (2010) 7191-7200.

[27] S. Saka, D. Kusdiana, Biodiesel fuel from rapeseed oil as prepared in supercritical methanol, Fuel, 80 (2001) 225-231.

[28] S.J. Yoo, H.-s. Lee, B. Veriansyah, J. Kim, J.-D. Kim, Y.-W. Lee, Synthesis of biodiesel from rapeseed oil using supercritical methanol with metal oxide catalysts, Bioresource Technology, 101 (2010) 8686-8689.

[29] N.C. Shin, Y.-H. Lee, Y.H. Shin, J. Kim, Y.-W. Lee, Synthesis of cobalt nanoparticles in supercritical methanol, Materials Chemistry and Physics, 124 (2010) 140-144.

[30] B. Veriansyah, J.-D. Kim, B.K. Min, J. Kim, Continuous synthesis of magnetite nanoparticles in supercritical methanol, Materials Letters, 64 (2010) 2197-2200.

[31] European Committee for Standardization (CEN), BS EN 14103:2003, Fat and oil derivatives - Fatty acid methyl esters (FAME) - Determination of ester and linolenic acid methyl ester contents.

[32] E.-S. Song, J.-w. Lim, H.-S. Lee, Y.-W. Lee, Transesterification of RBD palm oil using

supercritical methanol, The Journal of Supercritical Fluids, 44 (2008) 356-363.

[33] D. Kusdiana, S. Saka, Kinetics of transesterification in rapeseed oil to biodiesel fuel as treated in supercritical methanol, Fuel, 80 (2001) 693-698.

[34] A. Demirbaş, Biodiesel fuels from vegetable oils via catalytic and non-catalytic supercritical alcohol transesterifications and other methods: a survey, Energy Conversion and Management, 44 (2003) 2093-2109.

[35] B. Veriansyah, J.-D. Kim, B.K. Min, Y.H. Shin, Y.-W. Lee, J. Kim, Continuous synthesis of surface-modified zinc oxide nanoparticles in supercritical methanol, The Journal of Supercritical Fluids, 52 (2010) 76-83.

[36] M. Kim, H.-s. Lee, S.J. Yoo, Y.-S. Youn, Y.H. Shin, Y.-W. Lee, Simultaneous synthesis of biodiesel and zinc oxide nanoparticles using supercritical methanol, Fuel, 109 (2013) 279-284.

[37] H. Choi, B. Veriansyah, J. Kim, J.-D. Kim, J.W. Kang, Continuous synthesis of metal nanoparticles in supercritical methanol, The Journal of Supercritical Fluids, 52 (2010) 285-291.

[38] Shriver, Atkins, Inorganic Chemistry, Fourth ed., Oxford University Press, 2006.

[39] X. Luo, Z. Li, C. Yuan, Y. Chen, Polyol synthesis of silver nanoplates: The crystal growth mechanism based on a rivalrous adsorption, Materials Chemistry and Physics, 128 (2011) 77-82.

[40] J.N. Solanki, Z.V.P. Murthy, Highly monodisperse and sub-nano silver particles synthesis via microemulsion technique, Colloids and Surfaces A: Physicochemical and Engineering Aspects, 359 (2010) 31-38.

[41] J.P. Chen, L.L. Lim, Key factors in chemical reduction by hydrazine for recovery of precious metals, Chemosphere, 49 (2002) 363-370.

[42] X.M. Lin, C.M. Sorensen, K.J. Klabunde, G.C. Hadjipanayis, Temperature Dependence of Morphology and Magnetic Properties of Cobalt Nanoparticles Prepared by an Inverse Micelle Technique, Langmuir, 14 (1998) 7140-7146.

[43] K. Sue, N. Kakinuma, T. Adschiri, K. Arai, Continuous Production of Nickel Fine Particles by Hydrogen Reduction in Near-Critical Water, Industrial and Engineering Chemistry Research, 43 (2004) 2073-2078.

[44] S. Ohara, H. Hitaka, J. Zhang, M. Umetsu, T. Naka, T. Adschiri, Hydrothermal synthesis of cobalt nanoparticles in supercritical water, Funtai Oyobi Fummatsu Yakin/Journal of the Japan Society of Powder and Powder Metallurgy, 54 (2007) 635-638.

[45] G. Seong, S. Takami, T. Arita, K. Minami, D. Hojo, A.R. Yavari, T. Adschiri, Supercritical hydrothermal synthesis of metallic cobalt nanoparticles and its thermodynamic analysis, Journal of Supercritical Fluids, 60 (2011) 113-120.

[46] T. Arita, H. Hitaka, K. Minami, T. Naka, T. Adschiri, Synthesis of iron nanoparticle: Challenge to determine the limit of hydrogen reduction in supercritical water, Journal of Supercritical Fluids, 57 (2011) 183-189.

[47] B. Katryniok, H. Kimura, E. Skrzynska, J.-S. Girardon, P. Fongarland, M. Capron, R. Ducoulombier, N. Mimura, S. Paul, F. Dumeignil, Selective catalytic oxidation of glycerol: perspectives for high value chemicals, Green Chemistry, 13 (2011) 1960-1979.

국문 초록 (Abstract in Korean)

나노 크기의 물질은 특별하고 고유한 물성을 보유하고 있고 그렇기 때문에 광학, 전기, 자석, 촉매 등의 연구에 다양하게 응용할 수 있다. 산업적 용도의 나노 물질 생산은 일정한 입자 크기 유지, 생산 경제성, 환경 친화성, 재현성 등의 기준을 요구한다. 나노 물질을 합성하는 방법 중 가장 잘 알려진 방법은 화학적 합성법으로 인버스 마이셀이나 비수화 졸겔 반응 등이 있다. 이러한 화학적 합성법은 독성이 있는 유기 용매를 사용하고 반응 시간이 길며, 분리 정제 공정이 복잡하고 비효율적이고, 회분식 생산 방법이 유일한 생산 방법이다.

본 학위논문은 초임계 유체를 이용하여 금속과 금속산화물 나노 입자를 합성하는 내용을 보고한다. 연구의 목표는 원하는 금속 또는 금속산화물 나노 입자를 초임계 유체와 자연에서 얻을 수 있는 생물 재료를 이용하여 합성하는 것이다. 이런 환경 친화적인 공정의 장점은 원재료의 가격이 싸고, 반응시간이 짧으며, 반응이 단순하고, 분리 정제가 쉽다고, 연속식 플러그 흐름 생산법 적용이 가능하다는 점이다.

첫 장에서는 초임계 수와 콩기름 또는 팜유와 같은 식용유를 통해 세리아 나노결정을 수열합성하고 자체적으로 표면 개질하는 공정을 개발하였다. XRD 패턴으로 순수한 세리아가 합성 된 것을 확인하였고 TEM 분석을 통해 단일 결정이 생산 되었

고 이 단일 결정이 유기용매에 안정하게 분산 되는 것을 확인하였다. FT-IR 스펙트럼과 TGA 분석을 통해 유리 지방산이 세리아 표면에 화학적으로 흡착한 것을 확인하였다. 이 기술은 정제된 유리지방산보다 가격이 저렴하고 구하기 쉬운 식용유를 나노 입자의 표면 개질제로 사용하여 경제성을 확보했다는데 의미가 있다.

두번째 장에서는 초임계 메탄올을 이용하여 바이오디젤과 금속산화물의 동시 합성을 진행하였다. 사용한 금속의 전구체는 모두 금속 질산염이다. 동시 생산에서 생성된 금속산화물은 바이오디젤 합성 반응에서 촉매로도 작용하였다. 이러한 촉매 작용에 의하여 바이도디젤 생산 공정의 온도와 반응시간을 낮출 수 있었다. FAME의 최고 수율은 96.88%였고 이는 250 ˚C, 350 bar, 질산아연 3 oil wt% 의 조건에서 10분 동안 반응하여 얻을 수 있었다. FT-IR 분석으로 FAME 분자들이 동시 생성된 금속산화물의 표면에 화학적으로 흡착한 사실을 확인하였다. 동시 생산한 금속산화물 입자는 메탄올 단독으로 합성한 입자들보다 크기가 작았다. 이 기술은 기존의 초임계 메탄올을 이용하여 바이오디젤을 생산하는 공정보다 반응 온도와 시간을 단축시켜 경제적이고 금속산화물을 부산물로 얻는 장점도 가지고 있다.

세번째 장에서는 글리세롤을 환원제로 이용하여 초임계 수열 합성을 통해 금속을 환원시키는 공정에 대한 것이다. 공정 조건은 400 ˚C, 300 bar 이고 금속 원자에 따라 완벽히 환원이 되거나 부분적으로 환원이 되는 것을 확인하였다. 기존 수열합성에서는 금속을 환원시키기 위하여 개미산이나 하이드라진을 이용하는데, 이 두 물질

은 독성이 있고 취급이 위험하고 악취가 나며 가격이 비싸다. 반대로 글리세롤은 안전하고 가격이 싸기 때문에 나노 입자 수열 합성에 있어서 매우 환경친화적인 환원제이다. XRD 분석을 통해 은, 구리, 니켈은 완벽하게 환원이 되는 것을 확인하였다. 이와 반대로 코발트, 철, 망간의 경우 금속산화물로 부분적으로 환원이 되었는데, 여기서는 글리세롤이 항산화제로 작용한 것이다. 환원시킨 입자는 글리세롤을 넣지 않은 경우의 입자보다 크기가 작았다. 글리세롤은 냄새가 없고, 비가연성이며, 취급이 용이하고 환경친화적이고, 산업적으로 쉽게 취득할 수 있다. 이 공정은 수열 합성 환원에 있어서 가장 녹색 공정이라 할 수 있다.

본 논문에서 서술한 세 장은 금속, 금속산화물, 바이오디젤을 깨끗하고 안전하고 자연 생물 재료를 이용하여 합성하는 내용에 관한 것이다. 본 학위의 최종적인 목표는 초임계 유체를 이용하여 친환경 녹색 공정을 개발하고, 이에 따라 기존의 위험하고 독성이 있는 화학 전구체의 사용을 최소화하는데 있다.

주요어: 초임계 유체, 초임계 수, 초임계 메탄올, 금속, 금속산화물, 나노입자, 나노결정, 바이오디젤, FAME, 식용유, 글리세롤, 전이에스테르화, 수열 공정, 환원

서울대학교 대학원

화학생물공학부

김민수

학번: 2010-30245

List of Publications

1. **M. Kim**, H.-s. Lee, S.J. Yoo, Y.-S. Youn, Y.H. Shin, Y.-W. Lee, Simultaneous synthesis of biodiesel and zinc oxide nanoparticles using supercritical methanol, Fuel, 109 (2013) 279-284.

2. **M. Kim**, H.-s. Lee, Y. Shin, K. Ahn, Y.-S. Youn, J. Kim, Y.-W. Lee, Vegetable oil aided hydrothermal synthesis of cerium oxide nanocrystals, Korean J. Chem. Eng., 29 (2012) 1289-1291.

3. K.H. Ahn, Y.-H. Lee, **M. Kim**, H.-s. Lee, Y.-S. Youn, J. Kim, Y.-W. Lee, Effects of Surface Area of Titanium Dioxide Precursors on the Hydrothermal Synthesis of Barium Titanate by Dissolution–Precipitation, Industrial & Engineering Chemistry Research, 52 (2013) 13370-13376.

4. Y.-S. Youn, J.H. Oh, K.H. Ahn, **M. Kim**, J. Kim, Y.-W. Lee, Dissolution rate improvement of valsartan by low temperature recrystallization in compressed CO2: Prevention of excessive agglomeration, The Journal of Supercritical Fluids, 59 (2011) 117-123.

5. K. H. Ahn, N.-C. Shin, **M. Kim**, Y.-S. Youn, G. H. Hong, Y.-W. Lee, Synthesis of ceria nanoparticles using supercritical methanol with various surface modifiers, Korean Chem. Eng. Res., Vol. 50, No. 4, 678-683